Clinical Electroencephalography for Anesthesiologists

HHS Public Access

Author manuscript

Anesthesiology. Author manuscript; available in PMC 2015 October 01.

Published in final edited form as:

Anesthesiology. 2015 October ; 123(4): 937–960. doi:10.1097/ALN.0000000000000841.

Clinical Electroencephalography for Anesthesiologists Part I: Background and Basic Signatures

Patrick L. Purdon, Ph.D.[*], **Aaron Sampson, B.S.**[§], **Kara J. Pavone, B.S.**[§], and **Emery N. Brown, M.D., Ph.D.**[#]

[*]Associate Bioengineer, Department of Anesthesia, Critical Care and Pain Medicine, Massachusetts General Hospital, Boston, Massachusetts; Assistant Professor of Anaesthesia, Department of Anesthesia, Harvard Medical School, Boston, Massachusetts

[§]Research Assistant, Department of Anesthesia, Critical Care and Pain Medicine, Massachusetts General Hospital, Boston, Massachusetts

[#]Anesthetist, Department of Anesthesia, Critical Care and Pain Medicine, Massachusetts General Hospital, Boston, Massachusetts; Warren M. Zapol Professor of Anesthesia, Department of Anesthesia, Harvard Medical School, Boston, Massachusetts; Edward Hood Taplin Professor of Medical Engineering, Institute for Medical Engineering and Science and Harvard-Massachusetts Institute of Technology, Health Sciences and Technology Program, Professor of Computational Neuroscience, Department of Brain and Cognitive Sciences, Massachusetts Institute of Technology, Cambridge, Massachusetts

Abstract

The widely used electroencephalogram-based indices for depth-of-anesthesia monitoring assume that the same index value defines the same level of unconsciousness for all anesthetics. In contrast, we show that different anesthetics act at different molecular targets and neural circuits to produce distinct brain states that are readily visible in the electroencephalogram. We present a two-part review to educate anesthesiologists on use of the unprocessed electroencephalogram and its spectrogram to track the brain states of patients receiving anesthesia care. Here in Part I, we review the biophysics of the electroencephalogram, and the neurophysiology of the electroencephalogram signatures of three intravenous anesthetics: propofol, dexmedetomidine and ketamine; and four inhaled anesthetics: sevoflurane, isoflurane, desflurane and nitrous oxide. Later in Part II, we discuss patient management using these electroencephalogram signatures. Use of

Corresponding Authors: Patrick L. Purdon, Ph.D., Department of Anesthesia, Critical Care and Pain Medicine, Massachusetts General Hospital, 55 Fruit Street, GRB-444, Boston, Massachusetts, Tel: 617 726 7487, Fax: 617 726 1880. patrickp@nmr.mgh.harvard.edu.

DEPARTMENT AND INSTITUTION

Department of Anesthesia, Critical Care and Pain Medicine, Massachusetts General Hospital, Boston, Massachusetts

PRIOR PRESENTATION OF WORK

Drs. Purdon and Brown have summarized some of this work on the website www.anesthesiaeeg.com and have given several seminars on this topic in multiple venues during the last 2 years.

CONFLICTS OF INTERST

Masimo has signed an agreement with Massachusetts General Hospital to license the signal processing algorithms developed by Drs. Brown and Purdon for analysis of the electroencephalogram to track the brain states of patients receiving general anesthesia and sedation for incorporation into their brain function monitors.

these electroencephalogram signatures suggests a neurophysiologically-based paradigm for brain-state monitoring of patients receiving anesthesia care.

The Electroencephalogram and Brain Monitoring under General Anesthesia

Almost 80 years ago, Gibbs, Gibbs and Lenox demonstrated that systematic changes occur in the electroencephalogram and patient arousal level with increasing doses of ether or pentobarbital. They stated that "a practical application of these observations might be the use of electroencephalogram as a measure of the depth of anesthesia."[1] Several subsequent studies reported on the relationship between electroencephalogram activity and the behavioral states of general anesthesia.[2–6] Faulconer showed in 1949 that a regular progression of the electroencephalogram patterns correlated with the concentration of ether in arterial blood.[7] Linde and colleagues used the spectrum—the decomposition of the electroencephalogram signal into the power in its frequency components—to show that under general anesthesia the electroencephalogram was organized into distinct oscillations at particular frequencies.[8,9] Bickford and colleagues introduced the compressed spectral array or spectrogram to display the electroencephalogram activity of anesthetized patients over time as a three-dimensional plot (power by frequency versus time).[10,11] Fleming and Smith devised the density-modulated or density spectral array, the two-dimensional plot of the spectrogram for this same purpose.[12,13] Levy later suggested using multiple electroencephalogram features to track anesthetic effects.[14] Despite further documentation of systematic relationships among anesthetic doses, electroencephalogram patterns and patient arousal levels,[4,15–20] use of the unprocessed electroencephalogram and the spectrogram to monitor the states of the brain under general anesthesia and sedation never became a standard practice in anesthesiology.

Instead, since the 1990s, depth-of-anesthesia has been tracked using indices computed from the electroencephalogram and displayed on brain monitoring devices.[21–25] The indices have been developed by recording simultaneously the electroencephalogram and the behavioral responses to various anesthetic agents in patient cohorts.[26] Some of the indices have been derived by using regression methods to relate selected electroencephalogram features to the behavioral responses.[26–29] One index has been constructed by using classifier methods to derive a continuum of arousal levels from awake to profound unconsciousness from visually categorized electroencephalogram recordings.[30,31] Another index has been constructed by relating the entropy of the electroencephalogram signal—its degree of disorder—to the behavioral responses of the patients.[32,33] The indices are computed from the electroencephalogram in near-real-time and displayed on the depth-of-anesthesia monitor as values scaled from 0 to 100, with low values indicating greater depth of anesthesia. The algorithms used in many of the current depth-of-anesthesia monitors to compute the indices are proprietary.

Although the electroencephalogram-based indices have been in use for nearly 20 years, there are several reasons why they are not part of standard anesthesiology practice. First, use of electroencephalogram-based indices does not ensure that awareness under general anesthesia can be prevented.[34,35] Second, these indices, which have been developed from adult patient cohorts, are less reliable in pediatric populations.[36,37] Third, because the indices do not

relate directly to the neurophysiology of how a specific anesthetic exerts its effects in the brain, they cannot give an accurate picture of the brain's responses to the drugs. Finally, the indices assume that the same index value reflects the same level of unconsciousness for all anesthetics. This assumption is based on the observation that several anesthetics, both intravenous and inhaled agents, eventually induce slowing in the electroencephalogram oscillations at higher doses.[1,4,22] The slower oscillations are assumed to indicate a more profound state of general anesthesia. Two anesthetics whose electroencephalogram responses frequently lead clinicians to doubt index readings are ketamine[38,39] and nitrous oxide.[40–42] These agents are commonly associated with faster electroencephalogram oscillations that tend to increase the value of the indices at clinically accepted doses. Higher index values cause concern as to whether the patients are unconscious. At the other extreme, dexmedetomidine can produce profound slow electroencephalogram oscillations[43] and low index values consistent with the patient being profoundly unconscious. However, the patient can be easily aroused from what is a state of sedation rather than unconsciousness.[43,44]

These ambiguities in using electroencephalogram-based indices to define brain states under general anesthesia and sedation arise because different anesthetics act at different molecular targets and neural circuits to create different states of altered arousal,[45,46] and as we show, different electroencephalogram signatures.[43,47] The signatures are readily visible as oscillations in the unprocessed electroencephalogram and its spectrogram. We relate these oscillations to the actions of the anesthetics at specific molecular targets in specific neural circuits.

Therefore, we propose a new approach to brain monitoring of patients receiving general anesthesia or sedation: train anesthesiologists to recognize and interpret anesthetic-induced brain states defined by drug-specific neurophysiological signatures observable in the unprocessed electroencephalogram and the spectrogram. The new concept of defining the anesthetic state by using drug-specific electroencephalogram signatures that relate to molecular and neural circuit mechanisms of anesthetic action would allow anesthesiologists to make more detailed and accurate assessments than those based on electroencephalogram-based indices. The potential benefits of using the unprocessed electroencephalogram to monitor anesthetic states have been recently stated.[48,49] Current brain monitors display the unprocessed electroencephalogram and the spectrogram.[22,31,50]

To define anesthetic states in terms of drug-specific electroencephalogram signatures that relate to molecular and neural circuit mechanisms of anesthetic action, we synthesize different sources and levels of information: 1) formal behavioral testing along with simultaneous electroencephalogram recordings or human intracranial recordings during anesthetic administration; 2) clinical observations of behavior along with simultaneous electroencephalogram recordings during anesthetic administration; 3) the neurophysiology and the molecular pharmacology of how the anesthetics act at specific molecular targets in specific circuits; 4) the neurophysiology of altered states of arousal such as non-REM sleep, coma (medically induced, pathologic, hypothermia-induced), hallucinations and paradoxical excitation; 5) time-frequency analyses of high-density electroencephalogram recordings; and 6) mathematical modeling of anesthetic actions in neural circuits.

We present this new education paradigm in two parts. Here, in Part I, we review the basic neurophysiology of the electroencephalogram, and the neurophysiology and the electroencephalogram signatures of three intravenous anesthetics: propofol, dexmedetomidine and ketamine; and four inhaled anesthetics: sevoflurane, isoflurane, desflurane and nitrous oxide. We explain, where possible, how the anesthetics act at specific receptors in specific neural circuits to produce the observed electroencephalogram signatures. In Part II, we discuss how knowledge of the different electroencephalogram signatures may be used in patient management.

The Electroencephalogram: A Window into the Brain's Oscillatory State

Coordinated action potentials, or spikes, transmitted and received by neurons, are one of the fundamental mechanisms through which information is exchanged in the brain and central nervous system (fig. 1A).[51,52] Neuronal spiking activity generates extracellular electrical potentials,[53] composed primarily of post-synaptic potentials and neuronal membrane hyperpolarization (fig. 1A).[53,54] These extracellular potentials are often referred to as local field potentials. Populations of neurons often show oscillatory spiking and oscillatory local field potentials that are thought to play a primary role in coordinating and modulating communication within and among neural circuits.[52] Local field potentials produced in the cortex can be measured at the scalp as the electroencephalogram (fig. 1B).

The organization of the pyramidal neurons in the cortex favors the production of large local field potentials because the dendrites of the pyramidal neurons run parallel with each other and perpendicular to the cortical surface (fig. 1C). This geometry creates a biophysical transmitting antenna that generates large extracellular currents whose potentials can be measured through the skull and scalp as the electroencephalogram.[53,55,56] Subcortical regions, such as the thalamus (fig. 1D), produce much smaller potentials that are more difficult to detect at the scalp since the electric field decreases in strength as the square of the distance from its source.[56] However, because cortical and subcortical structures are richly interconnected, scalp electroencephalogram patterns reflect the states of both cortical and subcortical structures.[57] Thus, the electroencephalogram provides a window into the brain's oscillatory state.

A growing body of evidence suggests that anesthetics induce oscillations that alter or disrupt the oscillations produced by the brain during normal information processing.[19,20,57–63] These anesthesia-induced oscillations are readily visible in the electroencephalogram.

Data Analysis

To show unprocessed electroencephalogram recordings and their spectrograms computed with the same methods on comparable displays, we have taken examples from cases of patients receiving general anesthesia and sedation at our Institution. These data were recorded following a protocol approved by the Massachusetts General Hospital Human Research Committee to construct a database of electroencephalogram of recordings of patients receiving general anesthesia and sedation. Electroencephalograms were recorded using the Sedline monitor (Masimo Corporation, Irvine California). The Sedline electrode array records approximately at positions Fp1, Fp2, F7, and F8, with reference approximately

1 cm above Fpz and ground at Fpz. We required impedances less than 5kΩ in each channel. Our analyses use Fp1 as results were identical for Fp1 and Fp2. We also include analyses of human intracranial neurophysiology[60] and high-density electroencephalogram[20] from previous studies.

The spectrograms were computed using the multitaper method[64,65] from the unprocessed electroencephalogram signals recorded at a sampling frequency of 250 Hz. Individual spectra were computed in 3-sec windows with 0.5 sec overlap between adjacent windows. Multitaper spectral estimates have near optimal statistical properties[64,65] that substantially improve the clarity of spectral features. At present, no current electroencephalogram monitor displays multitaper spectra or spectrograms. However, we present multitaper spectra in this review in order to illustrate the EEG signatures of different anesthetic drugs with the greatest clarity.

Time-Domain and Spectral Measures of the Brain's Sedative and Anesthetic States

Many of the changes that occur in the brain with changes in anesthetic states can be readily observed in unprocessed electroencephalogram recordings (fig. 2). Different behavioral and neurophysiological states induced by anesthetics are associated with different electroencephalogram waveforms. For example, fig. 2 shows the electroencephalogram of the same patient in different states of propofol-induced sedation and unconsciousness.[20,65] These include the awake state (fig. 2A), paradoxical excitation (fig. 2B), a sedative state (fig. 2C), slow and alpha oscillation anesthetic state (fig. 2D), slow oscillation anesthetic state (fig. 2E), burst suppression (fig. 2F) and the isoelectric state (fig. 2G). Visualization and analysis of the unprocessed electroencephalogram is a form of time-domain analysis.[64,65] This approach is commonly used in sleep medicine and sleep research to define sleep states[66] and also in epileptology to characterize seizure states.[67]

Reading the frequencies and amplitudes from the unprocessed electroencephalogram in real-time in the operating room is challenging. If the frequencies of the oscillatory components were known, then it would be possible to design specific filters to extract these components (fig. 3A and B). The more practical and informative solution is to conduct a spectral analysis by computing the spectrum (fig. 3C) and the spectrogram (fig. 3D and 4).[64,65]

For a given segment of electroencephalogram data, the spectrum (fig. 3C) provides a decomposition of the segment into its frequency components usually computed by Fourier methods.[64,65] The advantage of the spectrum is that it shows the frequency decomposition of the electroencephalogram segment for all of the frequencies in a given range (fig. 3C) by plotting frequency on the x-axis and power on the y-axis. Power is commonly represented in decibels, defined as 10 times the log base 10 of the squared amplitude of a given electroencephalogram frequency component. Electroencephalogram power can differ by orders of magnitude across frequencies. Taking logarithms makes it easier to visualize on the same scale frequencies whose power differs by orders of magnitude. The spectrum of a given data segment is thus a plot of power $(10 \log_{10} (\text{amplitude})^2)$ by frequency.

The frequency bands in the spectrum are named following a generally accepted convention (Table 1). Changes in power in these bands can be used to track the changes in the brain's anesthetic states. In the signal in fig. 3A, the low frequency oscillation has a period of approximately 1 cycle/second or 1 Hertz (Hz) (Table 1, slow oscillation), whereas the period of the faster oscillation is at approximately 10 Hz (Table 1, alpha oscillation). The spectrum (fig. 3C) also shows that this signal has power in the delta range (1 to 4 Hz) and little to no power beyond 12 Hz.

In addition to these conventional frequency bands, two other spectral features are commonly reported in electroencephalogram analyses in anesthesiology: the median frequency (fig. 3C, vertical dashed line) and the spectral edge frequency (fig. 3C, vertical solid line). The median frequency is the frequency that divides the power in the spectrum in half[68,69] (fig. 3C), whereas the spectral edge frequency is the frequency below which 95% of the spectral power is located.[69] In other words, in the frequency range we use in our analyses of 0.1 to 30 Hz, half of the power in the spectrum lies below the median and 95% of the power lies below the spectral edge frequency. In fig. 3C, the median frequency and spectral edge frequency are respectively 3.4Hz and 15.9Hz, where the frequency range is 0.1 Hz to 30Hz. The median frequency and the spectral edge are displayed on commercial monitors and are useful clinically for tracking whether spectrogram power is shifting to lower (lower median frequency and spectral edge) or higher (higher median frequency and spectral edge) frequencies. As we discuss, the interpretations of these shifts are anesthetic dependent.

The spectrum displays the power content by frequency for only a single segment of electroencephalogram data. Use of the spectrum in electroencephalogram analyses during anesthesia care requires computing it on successive data segments. Successive computation of the spectrum across contiguous, often overlapping, segments of data is termed the spectrogram[64,65] (fig. 3D). The spectrogram makes it possible to display how the oscillations in the electroencephalogram change in time, with changes in the dosing of the anesthetics and/or the intensity of arousal-provoking stimuli. The spectrogram is a 3-dimensional structure (fig. 3D). However, it is plotted in two dimensions by placing time on the x-axis, frequency on the y-axis, and power through color coding on the z-axis (fig. 3E). As discussed earlier, this 2-dimensional plot of the spectrogram is termed the density spectral array.[12,13] whereas, the 3-dimensional plot of the spectrogram is termed the compressed spectral array (Fig. 3D).[10,22] We display the spectrogram as a density spectral array, and refer to it as the spectrogram.

Spectral analyses make it easier to visualize frequency content, especially oscillations, and to detect subtle changes in frequency structure. Nevertheless, it is important to know both the time-domain and spectral representations of a given behavioral or neurophysiological state induced by an anesthetic. We present both in our discussions in the following sections for commonly used intravenous and inhaled anesthetics.

Neurophysiology and Clinical Electrophysiology of Selected Intravenous Anesthetics

We review the neuropharmacology and clinical electrophysiology of propofol, dexmedetomidine and ketamine. For each anesthetic we discuss the putative mechanism through which its actions at specific molecular targets in specific neural circuits produce the electroencephalogram signatures and associated behavioral changes associated with its anesthetic state.

Molecular and Neural Circuit Mechanisms of Propofol

Propofol, the most widely administered anesthetic agent, is used as an induction agent for sedation and maintenance of general anesthesia. Low-dose propofol is frequently administered either as small boluses or by infusion for surgeries and diagnostic procedures that require only sedation.

The molecular mechanism of propofol has been well characterized. Propofol binds post-synaptically to $GABA_A$ receptors where it induces an inward chloride current which hyperpolarizes the post-synaptic neurons thus leading to inhibition.[70,71] Because the drug is lipid soluble and GABAergic inhibitory interneurons are widely distributed throughout the cortex, thalamus, brainstem and spinal cord, propofol induces sedation through its actions at multiple sites (fig. 4). In the cortex, propofol induces inhibition by enhancing GABA-mediated inhibition of pyramidal neurons.[71] Propofol decreases excitatory inputs from the thalamus to the cortex by enhancing GABAergic inhibition at the thalamic reticular nucleus, a network which provides important inhibitory control of thalamic output to the cortex. Because the thalamus and cortex are highly interconnected, the inhibitory effects of propofol lead not to inactivation of these circuits but rather to oscillations in the beta (figs. 3C and 5) and alpha (figs. 3D, 6 and 7) ranges. Propofol also enhances inhibition in the brainstem at the GABAergic projections from the pre-optic area of the hypothalamus to the cholinergic, monoaminergic and orexinergic arousal centers (fig. 4). Decreasing excitatory inputs from the thalamus and the brainstem to the cortex enhances hyperpolarization of cortical pyramidal neurons, an effect which favors the appearance of slow and delta oscillations on the electroencephalogram (figs. 5, 6 and 7).[20,60,72]

The Electroencephalogram Signatures of Propofol Sedation and Paradoxical Excitation are Beta-Gamma Oscillations

The electroencephalogram patterns seen during sedation are organized, regular beta-gamma oscillations (figs. 3C and 5) and slow-delta oscillations (fig. 5). The amplitudes of these oscillations are larger than those of the gamma oscillations seen in the awake electroencephalogram (fig. 2A). When general anesthesia has been maintained by a propofol infusion, a similar beta oscillation pattern is visible in patients after extubation as they lie quietly prior to transfer to the post-anesthesia care unit. A beta oscillation is also seen during paradoxical excitation (fig. 2B), the state of euphoria or dysphoria with movements that can occur when patients are sedated. The state is termed paradoxical because a dose of propofol intended to sedate results in excitation. Two mechanisms have been proposed to explain propofol induced paradoxical excitation. One involves $GABA_{A1}$-mediated inhibition of

inhibitory inputs from the globus pallidus to the thalamus leading to increased excitatory inputs from the thalamus to the cortex.[46] This mechanism is also the one through which the sedative zolpidem is postulated to induce arousal in minimally conscious patients.[73] The second mechanism, established in simulation studies, postulates that low-dose propofol induces transient blockade of slow potassium currents in cortical neurons.[74]

The Electroencephalogram Signatures of Propofol are Slow-Delta Oscillations on Induction

The electroencephalogram patterns observed during propofol general anesthesia depend critically on several factors, the most important of which is the rate of drug administration. When propofol is administered as a bolus for induction of general anesthesia the electroencephalogram changes within 10 to 30 seconds from an awake pattern with high-frequency, low-amplitude gamma and beta oscillations (fig. 2A) to patterns of high-amplitude slow and delta oscillations (fig 2E). The slow and delta oscillations appear in the spectrogram as increased power between 0.1 to 5 Hz (fig. 6A and 6B, between minutes 0 and 5) and in the time domain as high amplitude oscillations (fig. 6C, minute 5.5 and fig. 6D, minute 7.1) The electroencephalogram change is dramatic as the slow-oscillation amplitudes can be 5 to 20 times larger than the amplitudes of the gamma and beta oscillations seen in the electroencephalogram of an awake patient.[43]

The appearance of slow and delta oscillations (fig. 2, 6C, 6D) within seconds of administering propofol for induction of general anesthesia coincides with loss of responsiveness, loss of the oculocephalic reflex, apnea and atonia.[46,65] These electroencephalogram signatures and the clinical signs are consistent with a rapid action of the anesthetic in the brainstem. Following bolus administration, propofol quickly reaches the GABAergic inhibitory synapses emanating from the pre-optic area of the hypothalamus onto the major arousal centers in the brainstem and hypothalamus (fig. 4). Action of the anesthetic at these synapses inhibits the excitatory arousal inputs from the brainstem, favoring hyperpolarization of the cortex, the appearance of slow-delta oscillations on the electroencephalogram with loss of consciousness.[20,60,72] Loss of the oculocephalic reflex is consistent with the anesthetic acting at cranial nerve nuclei III, IV and VI in the midbrain and pons.[46,65] Apnea is most likely due to the drug's inhibition of the ventral and dorsal respiratory centers in the medulla and pons,[75] whereas the brainstem component of atonia is most likely due to inhibition of the pontine and medullary reticular nuclei.[46]

Administration of an additional propofol bolus, either prior to or following intubation, can result in either enhancement of the slow oscillation or the conversion of the slow oscillation into burst suppression (fig. 6B, minutes 7 to 14 and fig. 6D, minute 11.5) Burst suppression is a state of unconsciousness and profound brain inactivation in which the electroencephalogram shows periods of electrical activity alternating with periods of isoelectricity or electrical silence. In the spectrogram, burst suppression appears as vertical lines in the spectrogram (fig. 6B, minutes 7 to 14). When propofol is administered as an induction bolus, patients, particularly elderly patients, can enter burst suppression directly.[76]

As the effects of the bolus doses of propofol recede, the electroencephalogram evolves into slow-delta oscillation and alpha oscillation patterns (fig. 6A, minute 7 and fig. 6B, minute

15). The time of transition from the slow oscillations or burst suppression into a combined slow oscillation and alpha oscillation patterns depends on how profound the effect of the bolus dose was. Even if no additional propofol is administered after the first bolus, it can take several minutes for the transition to occur. The patient in fig. 6A received a second bolus dose of 50 mg at minute 5. An infusion of propofol was started at 100 mcg/kg/min. Her slow-delta oscillations did not evolve into the slow-delta and alpha oscillations until minute 7. In contrast, the patient in fig. 6B stayed in a state of burst suppression from minutes 7 to 14 after her two bolus doses of propofol. After the second bolus dose, she received no additional propofol or other anesthetics and transitioned into slow-delta and alpha oscillations (fig. 6B, minute 15 to 20 and fig. 6D, minutes 17). If following the bolus doses, propofol is administered as an infusion to maintain general anesthesia, the patient's electroencephalogram will continue to show the slow-delta and alpha oscillation patterns in the surgical plane (fig. 6A, minutes 9 to 26 and fig. 6C, minute 24).

Slow-Delta and Alpha Oscillations are Markers of Propofol-Induced Unconsciousness

Most brain function monitors used in anesthesiology record only a few channels of the electroencephalogram from the front of the head. An awake patient with eyes closed and a full set of scalp electroencephalogram electrodes will show the well-known eyes-closed alpha oscillations in the occipital areas (fig. 7A, Awake Baseline).[77] Concomitant with the transition to loss of consciousness and the appearance of the slow and alpha oscillations is the phenomenon of anteriorization, in which the power in the alpha and beta bands of the electroencephalogram shifts from the occipital area to the front of the head (fig. 7A, LOC and Unconsciousness).[15,19,20]

Although loss of consciousness due to propofol has a strong brainstem effect, maintenance of unconsciousness involves the brainstem and other brain centers. Studies of propofol-induced unconsciousness using a high-density (64-lead) electroencephalogram have shown that the alpha oscillations are highly coherent across the front of the head during unconsciousness (fig. 7A, Unconsciousness).[19,20] An explanation for this coherence is that propofol could be inducing an alpha oscillation within circuits linking the thalamus and the frontal cortex (fig. 7B).[57] In contrast, the slow oscillations are not coherent.[19,20] Studies of patients with intracortical electrodes also show that the slow oscillations induced by bolus administration of propofol are not coherent across the cortex (fig. 7C) and serve as a marker of phase-limited spiking activity in the cortex (fig. 7C).[60] We postulate that the highly organized coherent alpha oscillations most likely prevent normal communications between the thalamus and cortex, whereas the incoherent slow oscillations represent an impediment to normal intracortical communications.[20,57,60,78] Together, these two mechanisms likely contribute to the patient being unconscious when the slow and alpha oscillations are visible in the spectrogram of patients receiving propofol. These highly coherent alpha oscillations, incoherent slow oscillations and anteriorization most certainly contribute to the loss of frontal-parietal effective connectivity[78–80] that is also associated with propofol-induced loss of consciousness.

EEG Signatures of Emergence from Propofol General Anesthesia

When the propofol infusion is discontinued, and the patient is allowed to emerge, the slow and alpha oscillations dissipate and are gradually replaced by higher frequency beta and gamma oscillations that have lower amplitudes (fig. 6A, minute 25 to 30 and fig. 6B, minute 23 to 27).[20] In the spectrogram this gradual shift to higher frequency beta and gamma oscillations appears as a "zipper opening" pattern (fig. 6A, minute 25 to 30 and fig. 6B, minute 23 to 27). The decrease in the amplitude is shown by the shift in the spectrum from red to yellow. In the unprocessed electroencephalogram, this change is marked by a gradual increase in frequency and decrease in amplitude of the oscillations (fig. 6C, minute 24 and fig. 6D, minute 17). Simultaneously, there is dissipation of power in the slow and delta bands which appears in the time domain as a flattening of the unprocessed electroencephalogram. There is also reversal of anteriorization with emergence (fig. 7A, ROC and Awake Emergence) with loss of the coherent frontal alpha oscillations and return of the coherent occipital alpha oscillations.[20] The return of high-frequency power in the electroencephalogram is consistent with return of normal cortical activity and indirectly with return of normal thalamic and brainstem activity. Brainstem function returns in an approximate caudal (medulla and lower pons) to rostral (upper pons and midbrain) manner.[46,65] Breathing and gagging are controlled in the medulla and lower pons, whereas the corneal and oculocephalic reflexes are controlled in the upper pons and the midbrain.[46,65] Return of brainstem, thalamic and cortical activity are necessary to restore the awake state.

Burst Suppression and Medically-Induced Coma

When delivered in a sufficiently high dose, several anesthetics, including propofol, the barbiturates, and the inhaled ether drugs, induce burst suppression (figs. 3F, 6B, 6D, minute 11.5, 8A and 8B).[81–84] Burst suppression is induced by hypothermia for surgeries requiring total circulatory arrest[85] and by administering anesthetics in the intensive care unit for cerebral protection to treat intracranial hypertension or to treat status epilepticus.[84,86–88] This latter state is termed a medically-induced coma. If the patient is in burst suppression then, as the dose of the anesthetic is increased, the length of the suppression periods between the bursts increases. The dose can be increased to the point at which the electroencephalogram is isoelectric (fig. 2G). Within the bursts, the electroencephalogram can, in some cases, maintain the brain dynamics that were present prior to the start of burst suppression.[83,89,90] For example, if the patient is in a state of slow and alpha oscillations prior to the burst suppression, then the same pattern is present within the bursts (figs. 6B and 8A). In addition to deep general anesthesia, burst suppression is also observed in other conditions of profound brain inactivation including coma,[91] and in children with significantly compromised brain development.[92] The observation that multiple different mechanisms induce burst suppression are consistent with a recently proposed neuronal-metabolic mechanism of burst suppression.[83] Transient increases and decreases in extracellular calcium, leading to synaptic disfacilitation, could also play a role in determining suppression duration.[82]

The burst suppression ratio or suppression ratio is a time domain measure used to track quantitatively the level of burst suppression. The burst suppression ratio is a number

between 0 and 1 which measures the fraction of time in a given time interval that the electroencephalogram is suppressed.[93,94] The burst suppression ratio is displayed on some brain function monitors and is one of the measures used in electroencephalogram-based indices to assess depth-of-anesthesia.[95,96] A refinement of the burst suppression ratio, termed the burst suppression probability, has been recently developed (fig. 8C).[97] The burst suppression probability is a measure of the instantaneous probability of the brain being in a state of suppression that can be reliably computed using state-space methods and used to track burst suppression in real time and to implement control systems for medical coma.[97,98] A burst suppression probability of 0.5 means a 0.5 probability of being suppressed, whereas a burst suppression probability of 0.75 means a 0.75 probability of being suppressed.

Ketamine

Neural Circuit Mechanisms of Ketamine

Ketamine, an anesthetic adjunct and an analgesic, acts primarily by binding to NMDA receptors in the brain and spinal cord.[45] Ketamine is a channel blocker so that in order to be effective, the channel has to be open.[99] Because in general, the channels on inhibitory interneurons are more active than those on pyramidal neurons, ketamine at low to moderate doses has its primary effect on inhibitory interneurons (fig. 9A).[100,101] By blocking inputs to inhibitory interneurons, ketamine allows downstream excitatory neurons to become disinhibited or more active.[45] This is why cerebral metabolism increases with low doses of ketamine. Hallucinations, dissociative states, euphoria and dysphoria are common with low dose ketamine because brain regions, such as the cortex, hippocampus and the amygdala, continue to communicate but with less modulation and control by the inhibitory interneurons. Information is processed without proper coordination in space and time.[45,46] The hallucinatory effects are likely enhanced by disruption of dopaminergic neurotransmission in the prefrontal cortex due in part to increased glutamate activity at non-NMDA glutamate receptors.[102] Analgesia results most likely from the action of ketamine on glutamate NMDA receptors at the dorsal root ganglia, the first synapse of the pain pathway in the spinal cord where glutamate is the primary neurotransmitter (fig. 9A).[99] As the dose of ketamine is increased, the NMDA receptors on the excitatory glutamatergic neurons are also blocked and consciousness is lost.

The Electroencephalogram Signatures of Ketamine Sedation Are Beta and Gamma Oscillations

Given the preference of ketamine for NMDA receptors on inhibitory interneurons, whose inhibition results in increased cerebral metabolic rate, cerebral blood flow, and hallucinations,[103–105] it is no surprise that ketamine is associated with an active electroencephalogram pattern. When ketamine is administered alone in low dose, the electroencephalogram shows fast oscillations (fig. 9B and 9C) in the high beta, low gamma range at between 25 to 32 Hz. The beta-gamma oscillation did not start until 2 minutes after the initial ketamine dose. Compared with propofol and dexmedetomidine, discussed below in The Electroencephalogram Signatures of Dexmedetomidine are Slow-Delta Oscillations and Spindles, the ketamine slow oscillation is less regular (fig. 9C). The sixty-one year-old whose spectrogram is shown in fig. 9B required sedation and analgesia for change of a

vacuum dressing over a paniculectomy site. At minute 0, she received a 50 mg bolus of ketamine in two doses of 30 and 20 mg, 2 minutes apart. The dressing change started at minute 10. Five minutes after administering the 20 mg ketamine dose, the patient continued to breathe spontaneously, and was unresponsive to verbal commands and the nociceptive stimulation from the procedure. Although the beta and gamma oscillations lasted for only 27 minutes, the sedative effect of being unresponsive to verbal commands persisted for several minutes after the beta-gamma oscillations had disappeared.

Dexmedetomidine

Dexmedetomidine is used as a sedative in the intensive care unit and as a sedative and anesthetic adjunct in the operating room. Compared with propofol, patients are easily arousable when sedated with dexmedetomidine, with minimal to no respiratory depression. Unlike propofol and the benzodiazepines, dexmedetomidine cannot also be used as a hypnotic agent.

Neural Circuit Mechanisms of Dexmedetomidine

Dexmedetomidine alters arousal primarily through its actions on pre-synaptic α_2 adrenergic receptors on neurons projecting from the locus ceruleus. Binding of dexmedetomidine to the α_2 receptors hyperpolarizes locus coeruleus neurons decreasing norepinephrine release.[106–108] The behavioral effects of dexmedetomidine are consistent with this proposed mechanism of action.[109] Hyperpolarization of locus ceruleus neurons results in loss of inhibitory inputs to the pre-optic area of the hypothalamus (fig. 10A). The pre-optic area sends GABAergic and galanergic inhibitory projections to the major arousals centers in the midbrain, pons and hypothalamus (fig. 10A).[45,46,110] Hence, loss of the inhibitory inputs from the locus ceruleus results in sedation due to activation of these inhibitory pathways from the pre-optic area to the arousal centers. Activation of inhibitory inputs from the pre-optic area is postulated to be an essential component of how non-rapid eye movement sleep is initiated.[111,112] Sedation by dexmedetomidine is further enhanced due to blockage of pre-synaptic release of norepinephrine, leading to loss of excitatory inputs from the locus ceruleus to the basal forebrain, intralaminar nucleus of the thalamus, and cortex[113] and to thalamocortical connectivity.[114]

The Electroencephalogram Signatures of Dexmedetomidine are Slow-Delta Oscillations and Spindles

The relationship between the actions of dexmedetomidine in the pre-optic area and the initiation of non-rapid eye movement sleep is important to appreciate because it helps explain the similarities in the electroencephalogram patterns between this anesthetic and those observed in non-rapid eye movement sleep. Dexmedetomidine administered as a low-dose infusion induces a level of sedation in which the patient responds to minimal auditory or tactile stimulation. The electroencephalogram shows a combination of slow-delta oscillations with spindles, which are 9 to 15 Hz oscillations that occur in bursts lasting 1 to 2 seconds. (figs. 10B and 11, A and B).[43,44] In the frequency domain, the dexmedetomidine spindles appear as streaks in the high alpha and low beta bands between 9 to 15 Hz (fig. 11A). The spindles occur in a similar frequency range as the alpha oscillations seen with

propofol, but have much less power than the alpha oscillations (figs. 6A and 6B).[43] Because the color scales on the spectrograms in figs. 6A, 6B and 11A are the same, the plots provide an informative comparison of the amplitudes of the propofol alpha oscillations and the dexmedetomine spindles. The dexmedetomidine spindles closely resemble the spindles that define stage II non-rapid eye movement sleep.[43,44]

The slow-delta oscillations are apparent in the spectrogram as power from 0 to 4 Hz (fig. 11A). The 44 year-old, 59kg female patient, whose spectrogram and time domain traces are shown in figs. 11A and 11B, received a loading infusion of dexmedetomidine at 1 mcg/kg over 10 minutes, followed by a maintenance dexmedetomidine infusion of 0.65 mcg/kg/hour —a rate in the intermediate to high end of the sedative range—for the creation of a left forearm arteriovenous fistula for dialysis. During the surgery, the patient was sedated, meaning that she responded to verbal queries from the anesthesiologist and moved in response to nociceptive stimulation from the surgery.

When the rate of the dexmedetomidine infusion is increased, spindles disappear and the amplitude of the slow-delta oscillations increase (fig. 11C and 11D). This electroencephalogram pattern of slow-delta oscillations closely resembles non-rapid eye movement sleep stage III or slow-wave sleep.[66] The slow-delta oscillations appear again as intense power in the slow oscillation band (fig. 11D). The power in the slow oscillation band for the higher dose of dexmedetomidine (fig. 11C) is considerably stronger than the slow oscillations for the lower dose of dexmedetomine (fig. 11A). The spectrogram is that of a 48 year-old, 65kg female patient who received dexmedetomidine as a loading infusion of 1mcg/kg over 10 minutes and a maintenance infusion of 0.85 mcg/kg/hour for placement of a left forearm ateriovenous fistula. The intense slow-delta oscillation persisted for the duration of the procedure. During the surgery, the patient was sedated, meaning that she was unresponsive to verbal queries from the anesthesiologist and but moved in response to changes in the level of nociceptive stimulation from the procedure.

Propofol frontal alpha oscillations (fig. 7A), dexmedetomidine spindles[45] (fig. 11A and 11B) and sleep spindles[115] are all thought to be generated by thalamocortical loop mechanisms (fig. 7B and 10B). While the propofol frontal alpha oscillations are highly coherent and continuous in time[19,20,57], the sleep and dexmedetomidine spindles are brief and episodic.[43] Sleep spindles are a marker for non-rapid eye movement stage II sleep which is a state of unconsciousness that is less profound than non-rapid eye movement stage III or slow wave sleep.[66] Dexmedetomidine spindles are consistent with a light state of sedation.[43]

Propofol-induced slow oscillations likely result from decreased excitatory inputs to the cortex due to propofol's $GABA_A$-mediated inhibition arousal centers in the midbrain, pons and hypothalamus (fig. 4). Dexmedetomine-induced slow oscillations likely result from decreased excitatory inputs to the cortex due dexmedetomidine's disinhibition of the inhibitory circuits emanating from the pre-optic area of the hypothalamus to the arousal centers along with decreased adrenergically-mediated excitatory inputs to the basal forebrain, the intralaminar nucleus of the thalamus and to the cortex directly (fig. 10A). Propofol-induced slow oscillations gate brief periods of neuronal activity (fig. 7B).[60] In

contrast, sleep slow-wave oscillations are associated with brief interruptions in neuronal activity.[116] Similarly, both slow oscillations and spindles under dexmedetomidine are smaller than their counterparts under propofol, which may reflect a lower level of disruption in neuronal activity under dexemedetomidine compared to propofol.[43] Consequently, cortical and thalamo-cortical activity are likely to be more profoundly inhibited under propofol-induced unconsciousness compared to either slow-wave sleep or dexmedetomidine-induced sedation. This difference in cortical and thalamo-cortical activity suggests why patients can be aroused from sleep and dexmedetomidine-induced sedation, but not from propofol-induced unconsciousness.[43,60]

Clinical Electrophysiology of the Inhaled Anesthetics

Neurophysiological Mechanisms of Inhaled of Anesthetic Action

The principal inhaled anesthetics are the ether derivatives sevoflurane, isoflurane, and desflurane. The inhaled agents are total anesthetics in that they can maintain all of the required behavioral and physiological characteristics of general anesthesia without adjunct. In practice, the inhaled anesthetics are rarely used alone, but more commonly in conjunction with intravenous drugs, nitrous oxide and muscle relaxants to provide balanced general anesthesia which maximizes the desired effects while minimizing side effects. The inhaled agents are known to create their behavioral and physiological effects through binding at multiple targets in the brain and central nervous system including: binding to $GABA_A$ receptors and enhancing GABAergic inhibition; blockade of 2-pore potassium channels and HCN channels; and blocking glutamate release by binding to NMDA receptors.[70] Studies of minimal alveolar concentration (MAC) have shown that the muscle relaxant effects of the inhaled anesthetics are the result of direct action at one or more of these receptors and channels in the spinal cord.[117] This mechanism is also consistent with the observation that spinal cord motor evoked potentials are difficult to record in patients receiving anesthetic concentrations of an ether anesthetic.[118]

Gibbs, Gibbs and Lennox showed that the electroencephalogram of patients receiving ether show slow-delta oscillations and alpha oscillations at surgical levels of general anesthesia.[1] When sevoflurane is administered at sub-MAC concentrations to achieve surgical levels of general anesthesia the EEG shows slow-delta oscillations and coherent alpha oscillations similar to propofol.[47] This observation suggests that for sevoflurane, as for propofol, enhanced GABAergic inhibition may be its dominant mechanism of action.[47] However, unlike propofol, sevoflurane also shows a small coherent theta oscillation,[47] which may reflect one of its non-GABAergic mechanisms.

The Electroencephalogram Signatures of Sevoflurane, Isoflurane and Desflurane are Alpha, Slow-Delta and Theta Oscillations

At sub-MAC concentrations, sevoflurane shows strong alpha and slow-delta oscillations (fig. 12, A–D) that closely resemble those of propofol (fig. 6). As the concentration of sevoflurane is increased to MAC levels and above, a strong theta oscillation appears creating a distinctive pattern of evenly distributed power from the slow oscillation range up through the alpha range (fig. 12, A and C). This approximately equal power from the slow oscillation

range through to the alpha range (fig. 12, A and C) is typical during maintenance with sevoflurane at or above MAC. The theta oscillation power appears to fill in between the slow-delta and alpha oscillation power. As the concentration of sevoflourane is decreased, the theta oscillations dissipate first. This is evident in fig. 12A as the theta oscillations dissipate when the concentration of sevoflurane is lowered. On emergence, as in the case of propofol (fig. 6A, minute 27 and 6B, minute 25), the alpha oscillations transition to lower amplitude beta and gamma oscillations (fig. 12A, minute 180). At the same time, the slow and delta oscillations dissipate. The loss of the alpha and slow-delta oscillation power again appears in the spectrogram as a zipper opening pattern.

Isoflurane (fig. 12E and 12F) and desflurane (fig. 12G and 12H) have similar patterns to sevoflurane (fig. 12 C–D). At sub-MAC concentrations, they also show strong alpha and slow-delta oscillations. When the concentration of isoflurane or desflurane is increased to MAC levels and above, a theta oscillation fills in between the delta and alpha bands (fig. 12E, minute 30 and 12G, minute 28). As in the case of sevoflurane, on emergence from isoflurane and oxygen or desflurane and oxygen anesthesia, there is loss of the theta oscillation power, followed by dissipation of alpha and slow-delta oscillation power, and reappearance of the power in the beta and gamma bands (fig. 12E, minutes 78 to 80 and 12 G, minutes 85 to 90). These observations suggest, that by analogy with sevoflurane, enhanced GABAergic inhibition is likely a primary but not the only mechanism through which isoflurane and desflurane induce their anesthetic states. This relationship between MAC and theta oscillations is useful clinically. The appearance of theta oscillations indicates a more profound state of unconsciousness and immobility for an inhaled ether anesthetic.

As with propofol, burst suppression can be induced by administering a sufficiently high dose of any one of the inhaled ether anesthetic drugs.[81,84]

High-Amplitude Slow-Delta Oscillations Mark the Transition to High-Flow Nitrous Oxide

Nitrous oxide has been used as a sedative and as an anesthetic since the late 1800s.[3,119] Today, it is most often used as an anesthetic adjunct because, unlike the ether anesthetics, nitrous oxide is not sufficiently potent by itself to produce general anesthesia. Attempts to administer sufficient doses of only nitrous oxide to produce unconsciousness predictably result in nausea and vomiting.[41] Unlike the ether anesthetics, administering nitrous oxide with oxygen is not commonly thought to produce slow and alpha oscillations. Instead, nitrous oxide is associated with prominent beta and gamma[40] oscillations and possibly, with a relative decrease in power in the slow and delta oscillation bands.[41]

A common practice at our institution is to use an inhaled ether anesthetic with oxygen for maintenance of general anesthesia and to switch to a high concentration of nitrous oxide with oxygen with high total flow rates near the end of the case to hasten the patient's emergence. In this situation, a distinctive electroencephalogram pattern appears with the transition to nitrous oxide. It is illustrated in fig. 13. In anticipation of emergence, a 34 year-old patient was maintained on 0.5% isoflurane and 58% oxygen during the last minutes of a laprascopic cholecystectomy. At minute 82 the anesthetic was switched to 0.2% isoflurane, 75% nitrous oxide and 24% oxygen. With the switch, the total flow rate was increased from

3 to 7 liters per minute. Two minutes after the switch, the power in the slow, delta and alpha bands begins to decline (fig. 13A, minute 84). Four minutes following the switch, a profound slow-delta oscillation appears in the electroencephalogram (fig. 13A, minute 86 and 13B, minute 86). These slow-delta oscillations dominate with near loss of all power above 5Hz for approximately 4 minutes (fig. 13, minutes 86 to 90, blue area in the spectrogram) before they evolve to the beta-gamma oscillations that are more commonly associated with nitrous oxide (fig. 13A, minute 90 and 13B, minute 90). The appearance of the beta-gamma oscillations and the loss of the slow-delta oscillations take place from minutes 90 to 94. The patient was extubated at minute 110 (not shown).

The appearance of slow-delta oscillations we commonly observe in the switch from one of the ether anesthetics, halothane or propofol to a high concentration (> 70%) nitrous oxide has been previously reported.[120,121] The slow-delta oscillations tend to be transient[120,121] and the beta-gamma oscillations usually reported with nitrous oxide[40,41] appear the slow-delta oscillations dissipate. These slow-delta oscillations are noticeably different from the slow-waves seen during propofol induction (fig. 6) and during deep dexmedetomidine sedation (fig. 11D) in that they are accompanied by a substantial reduction in spectral power at all frequencies above 10 Hz (fig. 13A minutes 86 to 90). Although the mechanism of this slow oscillation is unknown, one possible explanation is blockade of NMDA-receptor mediated excitatory inputs from the parabrachial nucleus and the median pontine reticular formation to the basal forebrain and to the thalamus.[122] The beta-gamma oscillations may have a mechanism similar to that of ketamine (fig. 9B) whose increased beta-gamma activity depends critically on NMDA-mediated inactivation of inhibitory interneurons.[45]

Discussion

Anesthesiologists administer selected combinations of drugs to create the anesthetic state best suited for the patient and the given surgical or diagnostic procedure. A growing body of evidence suggests that the behavioral effects of the anesthetics are due to neural oscillations induced by their actions at specific molecular targets in specific neural circuits. Anesthesia-induced oscillations are 5 to 20 times larger than normal brain oscillations, likely disrupt normal brain communication (fig. 1) and are readily visible in the unprocessed electroencephalogram (fig. 2) and its spectrogram (fig. 3). Therefore, for three widely used intravenous anesthetics—propofol, ketamine and dexmedetomidine—we related the electroencephalogram signatures to the molecular targets and the neural circuits in the brain at which these drugs most likely act (figs. 4–11). For the inhaled ether-derived anesthetics sevoflurane, isoflurane and desflurane, we observed that, with the exception of the theta oscillations that appear around 1 MAC and beyond, their electroencephalogram patterns during maintenance and emergence closely resemble those seen in propofol (fig. 12). Nitrous oxide is known to be associated with increased beta and gamma oscillations and likely decreased slow-delta oscillations. However, we demonstrated that nitrous oxide also produces profound slow-delta oscillations during the transition from an inhaled ether anesthetic (fig. 13).

In contrast to brain state monitoring based on the electroencephalogram-derived indices, which assume that the same index value defines for any anesthetic the same level of

unconsciousness, the unprocessed electroencephalogram and the spectrogram define a broader range of brain states. Therefore, under our paradigm, their use should enable a more nuanced characterization of brain states guided by mechanistic insights. Our paradigm for brain state monitoring differs also from that used by neurologists and clinical neurophysiologists. These clinicians commonly use unprocessed electroencephalogram patterns to identify seizures in the intensive care unit[123,124], to characterize evoked potentials[123], to detect ischemia during neurophysiological monitoring in the operating room[125] or to characterize sleep stages.[126] Their paradigm relies on identifying patterns in the unprocessed electroencephalogram to diagnose seizures or ischemia irrespective of the anesthetic. To do so, clinical neurophysiologists frequently ask anesthesiologists to reduce or not use certain anesthetics, e.g. not to use ether anesthetics during spinal cord monitoring, to facilitate detection of clinically significant changes in unprocessed electroencephalogram patterns.[127] Hence, the neurologist's paradigm does not require understanding the electroencephalogram signatures of the anesthetics.

Our paradigm synthesizes research from the last 80 years. Gibbs, Gibbs and Lennox showed that under general anesthesia electroencephalograms patterns changed with level of unconsciousness.[1] Several investigators showed that different anesthetics have different electroencephalogram patterns and that these patterns were visible in the spectra of the electroencephalogram[10,12–14,22]. In 1959, Martin, Faulconer and Bickford wrote, "The big question, of course, remains unanswered; namely, do the electroencephalographic patterns defined in the several classifications presented constitute a valid measure of depth of anesthesia. We believe that this question unanswerable until a precise definition of 'depth of anesthesia' is made."[6] Relating the electroencephalogram patterns to the mechanisms was not possible at the time because lipid solubility was the primary theory of anesthetic mechanisms. The concept that anesthetics bind to specific molecular targets was not promulgated until 1984[128] and the detailed neural circuit descriptions of how anesthetic actions at specific molecular targets could lead to altered states of arousal were not reported until more than 25 years later.[45,46] In recent years, more has been learned about the biophysics of the electroencephalogram[53] and about how altered states of arousal induced by anesthetics relate to electroencephalogram activity.[19,20,43,47,57,60] Hence, it is now possible to link electroencephalogram signatures to anesthetic state and the actions of the drugs at specific molecular targets and in specific neural circuits (fig. 14).

Today, the unprocessed electroencephalogram and the spectrogram are displayed on several brain monitors.[31,50,129] Accurate spectral analyses are required to track accurately the anesthetic effects. For this reason, we computed our spectrograms using multitaper spectral methods. For a given data length, multitaper methods have been shown to be the optimal non-parametric spectral techniques in the sense of giving the spectral estimates with the highest resolution and the lowest variance.[64,65,130] As a result, the multitaper methods make it easier to identify the spectral features of anesthetic-specific signatures.

For the information we have covered in Part I to be useful in the management of patients receiving general anesthesia and sedation, it is important to describe how the electroencephalogram patterns change as different drugs are combined since this is the more common scenario in anesthesiology practice. The effects of combinations of anesthetics on

the electroencephalogram will be the topic of Part II. An animated version of portions of Parts I and II are available at AnesthesiaEEG.com. In Part III we will review the neurological examination for anesthesiologists.

Acknowledgments

DISCLOSURE OF FUNDING: Supported by grants DP1-OD003646 (to ENB) DP2-OD006454 (to PLP) and TR01-GM104948 (to ENB) from the National Institutes of Health, Bethesda, Maryland and funds from the Department of Anesthesia, Critical Care and Pain Medicine, Massachusetts General Hospital, Boston, Massachusetts.

References

1. Gibbs FA, Gibbs LE, Lennox WG. Effects on the electroencephalogram of certain drugs which influence nervous activity. Arch Intern Med. 1937; 60:154–66.
2. Faulconer, A.; Bickford, RG. Electroencephalography in anesthesiology. Springfield, Ill.: Thomas; 1960.
3. Faulconer A, Pender JW, Bickford RG. The influence of partial pressure of nitrous oxide on the depth of anesthesia and the electro-encephalogram in man. Anesthesiology. 1949; 10:601–9. [PubMed: 18147751]
4. Kiersey DK, Bickford RG, Faulconer A Jr. Electro-encephalographic patterns produced by thiopental sodium during surgical operations; description and classification. Br J Anaesth. 1951; 23:141–52. [PubMed: 14848401]
5. Galla SJ, Rocco AG, Vandam LD. Evaluation of the traditional signs and stages of anesthesia: an electroencephalographic and clinical study. Anesthesiology. 1958; 19:328–38. [PubMed: 13533914]
6. Martin JT, Faulconer A Jr, Bickford RG. Electroencephalography in anesthesiology. Anesthesiology. 1959; 20:359–76. [PubMed: 13650223]
7. Faulconer A Jr. Correlation of concentrations of ether in arterial blood with electro-encephalographic patterns occurring during ether-oxygen and during nitrous oxide, oxygen and ether anesthesia of human surgical patients. Anesthesiology. 1952; 13:361–9. [PubMed: 14943989]
8. Bart AJ, Homi J, Linde HW. Changes in power spectra of electroencephalograms during anesthesia with fluroxene, methoxyflurane and ethrane. Anesth Analg. 1971; 50:53–63. [PubMed: 5100243]
9. Findeiss JC, Kien GA, Huse KO, Linde HW. Power spectral density of the electroencephalogram during halothane and cyclopropane anesthesia in man. Anesth Analg. 1969; 48:1018–23. [PubMed: 5391378]
10. Bickford RG, Fleming N, Billinger T. Compression of EEG data. Trans Am Neurol Assoc. 1971; 96:118–22. [PubMed: 5159064]
11. Myers RR, Stockard JJ, Fleming NI, France CJ, Bickford RG. The use of on-line telephonic computer analysis of the E.E.G. in anaesthesia. Br J Anaesth. 1973; 45:664–70. [PubMed: 4730159]
12. Fleming RA, Smith NT. An inexpensive device for analyzing and monitoring the electroencephalogram. Anesthesiology. 1979; 50:456–60. [PubMed: 453564]
13. Levy WJ, Shapiro HM, Maruchak G, Meathe E. Automated EEG processing for intraoperative monitoring: a comparison of techniques. Anesthesiology. 1980; 53:223–36. [PubMed: 7425336]
14. Levy WJ. Intraoperative EEG patterns: implications for EEG monitoring. Anesthesiology. 1984; 60:430–4. [PubMed: 6711855]
15. Tinker JH, Sharbrough FW, Michenfelder JD. Anterior shift of the dominant EEG rhythm during anesthesia in the Java monkey: correlation with anesthetic potency. Anesthesiology. 1977; 46:252–9. [PubMed: 402870]
16. John ER, Prichep LS, Kox W, Valdes-Sosa P, Bosch-Bayard J, Aubert E, Tom M, di Michele F, Gugino LD. Invariant reversible QEEG effects of anesthetics. Conscious Cogn. 2001; 10:165–83. [PubMed: 11414713]

17. Gugino LD, Chabot RJ, Prichep LS, John ER, Formanek V, Aglio LS. Quantitative EEG changes associated with loss and return of consciousness in healthy adult volunteers anaesthetized with propofol or sevoflurane. Br J Anaesth. 2001; 87:421–8. [PubMed: 11517126]
18. Feshchenko VA, Veselis RA, Reinsel RA. Propofol-induced alpha rhythm. Neuropsychobiology. 2004; 50:257–66. [PubMed: 15365226]
19. Cimenser A, Purdon PL, Pierce ET, Walsh JL, Salazar-Gomez AF, Harrell PG, Tavares-Stoeckel C, Habeeb K, Brown EN. Tracking brain states under general anesthesia by using global coherence analysis. Proc Natl Acad Sci U S A. 2011; 108:8832–7. [PubMed: 21555565]
20. Purdon PL, Pierce ET, Mukamel EA, Prerau MJ, Walsh JL, Wong KF, Salazar-Gomez AF, Harrell PG, Sampson AL, Cimenser A, Ching S, Kopell NJ, Tavares-Stoeckel C, Habeeb K, Merhar R, Brown EN. Electroencephalogram signatures of loss and recovery of consciousness from propofol. Proc Natl Acad Sci U S A. 2013; 110:E1142–51. [PubMed: 23487781]
21. Schneider G, Gelb AW, Schmeller B, Tschakert R, Kochs E. Detection of awareness in surgical patients with EEG-based indices–bispectral index and patient state index. Br J Anaesth. 2003; 91:329–35. [PubMed: 12925469]
22. Rampil IJ. A primer for EEG signal processing in anesthesia. Anesthesiology. 1998; 89:980–1002. [PubMed: 9778016]
23. Palanca BJ, Mashour GA, Avidan MS. Processed electroencephalogram in depth of anesthesia monitoring. Curr Opin Anaesthesiol. 2009; 22:553–9. [PubMed: 19652597]
24. Bol C, Danhof M, Stanski DR, Mandema JW. Pharmacokinetic-pharmacodynamic characterization of the cardiovascular, hypnotic, EEG and ventilatory responses to dexmedetomidine in the rat. J Pharmacol Exp Ther. 1997; 283:1051–8. [PubMed: 9399976]
25. Barnard JP, Bennett C, Voss LJ, Sleigh JW. Can anaesthetists be taught to interpret the effects of general anaesthesia on the electroencephalogram? Comparison of performance with the BIS and spectral entropy. Br J Anaesth. 2007; 99:532–7. [PubMed: 17652076]
26. Kearse LA Jr, Manberg P, Chamoun N, deBros F, Zaslavsky A. Bispectral analysis of the electroencephalogram correlates with patient movement to skin incision during propofol/nitrous oxide anesthesia. Anesthesiology. 1994; 81:1365–70. [PubMed: 7992904]
27. Glass PS, Bloom M, Kearse L, Rosow C, Sebel P, Manberg P. Bispectral analysis measures sedation and memory effects of propofol, midazolam, isoflurane, and alfentanil in healthy volunteers. Anesthesiology. 1997; 86:836–47. [PubMed: 9105228]
28. Prichep LS, Gugino LD, John ER, Chabot RJ, Howard B, Merkin H, Tom ML, Wolter S, Rausch L, Kox WJ. The Patient State Index as an indicator of the level of hypnosis under general anaesthesia. Br J Anaesth. 2004; 92:393–9. [PubMed: 14742326]
29. Drover D, Ortega HR. Patient state index. Best Pract Res. Clin Anaesthesiol. 2006; 20:121–8.
30. Schultz B, Kreuer S, Wilhelm W, Grouven U, Schultz A. The Narcotrend monitor. Development and interpretation algorithms. Anaesthesist. 2003; 52:1143–8. [PubMed: 14691627]
31. Kreuer S, Wilhelm W. The Narcotrend monitor. Best Pract Res Clin Anaesthesiol. 2006; 20:111–9. [PubMed: 16634418]
32. Viertio-Oja H, Maja V, Sarkela M, Talja P, Tenkanen N, Tolvanen-Laakso H, Paloheimo M, Vakkuri A, Yli-Hankala A, Merilainen P. Description of the Entropy algorithm as applied in the Datex-Ohmeda S/5 Entropy Module. Acta Anaesthesiol Scand. 2004; 48:154–61. [PubMed: 14995936]
33. Jantti V, Alahuhta S. Spectral entropy–what has it to do with anaesthesia, and the EEG? Br J Anaesth. 2004; 93:150–1. author reply 151–2. [PubMed: 15192005]
34. Avidan MS, Zhang L, Burnside BA, Finkel KJ, Searleman AC, Selvidge JA, Saager L, Turner MS, Rao S, Bottros M, Hantler C, Jacobsohn E, Evers AS. Anesthesia awareness and the bispectral index. N Engl J Med. 2008; 358:1097–108. [PubMed: 18337600]
35. Avidan MS, Jacobsohn E, Glick D, Burnside BA, Zhang L, Villafranca A, Karl L, Kamal S, Torres B, O'Connor M, Evers AS, Gradwohl S, Lin N, Palanca BJ, Mashour GA, Group B-RR. Prevention of intraoperative awareness in a high-risk surgical population. N Engl J Med. 2011; 365:591–600. [PubMed: 21848460]

36. Samarkandi AH. The bispectral index system in pediatrics–is it related to the end-tidal concentration of inhalation anesthetics? Middle East J Anesthesiol. 2006; 18:769–78. [PubMed: 16749571]

37. Tirel O, Wodey E, Harris R, Bansard JY, Ecoffey C, Senhadji L. Variation of bispectral index under TIVA with propofol in a paediatric population. Br J Anaesth. 2008; 100:82–7. [PubMed: 18070785]

38. Hayashi K, Tsuda N, Sawa T, Hagihira S. Ketamine increases the frequency of electroencephalographic bicoherence peak on the alpha spindle area induced with propofol. Br J Anaesth. 2007; 99:389–95. [PubMed: 17621599]

39. Tsuda N, Hayashi K, Hagihira S, Sawa T. Ketamine, an NMDA-antagonist, increases the oscillatory frequencies of alpha-peaks on the electroencephalographic power spectrum. Acta Anaesthesiol Scand. 2007; 51:472–81. [PubMed: 17378787]

40. Yamamura T, Fukuda M, Takeya H, Goto Y, Furukawa K. Fast oscillatory EEG activity induced by analgesic concentrations of nitrous oxide in man. Anesth Analg. 1981; 60:283–8. [PubMed: 7194592]

41. Foster BL, Liley DT. Nitrous oxide paradoxically modulates slow electroencephalogram oscillations: implications for anesthesia monitoring. Anesth Analg. 2011; 113:758–65. [PubMed: 21788312]

42. Foster BL, Liley DT. Effects of nitrous oxide sedation on resting electroencephalogram topography. Clin Neurophysiol. 2013; 124:417–23. [PubMed: 22968005]

43. Akeju O, Pavone KJ, Westover MB, Vazquez R, Prerau MJ, Harrell PG, Hartnack KE, Rhee J, Sampson AL, Habeeb K, Lei G, Pierce ET, Walsh JL, Brown EN, Purdon PL. A comparison of propofol- and dexmedetomidine-induced electroencephalogram dynamics using spectral and coherence analysis. Anesthesiology. 2014; 121:978–89. [PubMed: 25187999]

44. Huupponen E, Maksimow A, Lapinlampi P, Sarkela M, Saastamoinen A, Snapir A, Scheinin H, Scheinin M, Merilainen P, Himanen SL, Jaaskelainen S. Electroencephalogram spindle activity during dexmedetomidine sedation and physiological sleep. Acta Anaesthesiol Scand. 2008; 52:289–94. [PubMed: 18005372]

45. Brown EN, Purdon PL, Van Dort CJ. General anesthesia and altered states of arousal: A systems neuroscience analysis. Annu Rev Neurosci. 2011; 34:601–28. [PubMed: 21513454]

46. Brown EN, Lydic R, Schiff ND. General anesthesia, sleep, and coma. N Engl J Med. 2010; 363:2638–50. [PubMed: 21190458]

47. Akeju O, Westover MB, Pavone KJ, Sampson AL, Hartnack KE, Brown EN, Purdon PL. Effects of sevoflurane and propofol on frontal electroencephalogram power and coherence. Anesthesiology. 2014; 121:990–8. [PubMed: 25233374]

48. Kertai MD, Whitlock EL, Avidan MS. Brain monitoring with electroencephalography and the electroencephalogram-derived bispectral index during cardiac surgery. Anesth Analg. 2012; 114:533–46. [PubMed: 22253267]

49. Bennett C, Voss LJ, Barnard JP, Sleigh JW. Practical use of the raw electroencephalogram waveform during general anesthesia: the art and science. Anesth Analg. 2009; 109:539–50. [PubMed: 19608830]

50. Drover DR, Schmiesing C, Buchin AF, Ortega HR, Tanner JW, Atkins JH, Macario A. Titration of sevoflurane in elderly patients: blinded, randomized clinical trial, in non-cardiac surgery after beta-adrenergic blockade. Journal of clinical monitoring and computing. 2011; 25:175–81. [PubMed: 21830049]

51. Kandel, ER. Nerve Cells and Behavior, Principles of Neural Science. 5th. New York: McGraw-Hill; 2013. p. 19-35.

52. Buzsaáki, G. Synchronization by Oscillation, Rhythms of the Brain. Oxford, New York: Oxford University Press; 2006. p. 136-174.

53. Buzsaki G, Anastassiou CA, Koch C. The origin of extracellular fields and currents–EEG, ECoG, LFP and spikes. Nat Rev Neurosci. 2012; 13:407–20. [PubMed: 22595786]

54. Hughes SW, Crunelli V. Thalamic mechanisms of EEG alpha rhythms and their pathological implications. The Neuroscientist. 2005; 11:357–72. [PubMed: 16061522]

55. Purves, D.; Augustine, GJ.; Hall, WC.; Lamantia, A.; McNamara, JO.; White, LE. Neuroscience. 4th. Sunderland, Massachusetts: Sinauer Associates, Inc; 2008. p. 715-717.
56. Hamalainen M, Hari R, Ilmoniemi RJ, Knuutila J, Lounasmaa OV. Magnetoencephalography–theory, instrumentation, and applications to noninvasive studies of the working human brain. Reviews of Modern Physics. 1993; 65:413–497.
57. Ching S, Cimenser A, Purdon PL, Brown EN, Kopell NJ. Thalamocortical model for a propofol-induced alpha-rhythm associated with loss of consciousness. Proc Natl Acad Sci U S A. 2010; 107:22665–70. [PubMed: 21149695]
58. Supp GG, Siegel M, Hipp JF, Engel AK. Cortical hypersynchrony predicts breakdown of sensory processing during loss of consciousness. Current biology. 2011; 21:1988–93. [PubMed: 22100063]
59. Chauvette S, Crochet S, Volgushev M, Timofeev I. Properties of slow oscillation during slow-wave sleep and anesthesia in cats. Journal of Neuroscience. 2011; 31:14998–5008. [PubMed: 22016533]
60. Lewis LD, Weiner VS, Mukamel EA, Donoghue JA, Eskandar EN, Madsen JR, Anderson WS, Hochberg LR, Cash SS, Brown EN, Purdon PL. Rapid fragmentation of neuronal networks at the onset of propofol-induced unconsciousness. Proceedings of the National Academy of Sciences of the United States of America. 2012; 109:E3377–86. [PubMed: 23129622]
61. Li D, Voss LJ, Sleigh JW, Li X. Effects of volatile anesthetic agents on cerebral cortical synchronization in sheep. Anesthesiology. 2013; 119:81–8. [PubMed: 23508217]
62. Wang K, Steyn-Ross ML, Steyn-Ross DA, Wilson MT, Sleigh JW. EEG slow-wave coherence changes in propofol-induced general anesthesia: experiment and theory. Front Syst Neurosci. 2014; 8:215. [PubMed: 25400558]
63. Vizuete JA, Pillay S, Ropella KM, Hudetz AG. Graded defragmentation of cortical neuronal firing during recovery of consciousness in rats. Neuroscience. 2014; 275:340–51. [PubMed: 24952333]
64. Mitra, PP.; Bokil, H. Observed Brain Dynamics. New York: Oxford University Press; 2008.
65. Babadi B, Brown EN. A review of multitaper spectral analysis. IEEE Trans Biomed Eng. 2014; 61:1555–64. [PubMed: 24759284]
66. McCarley RW. Neurobiology of REM and NREM sleep. Sleep Med. 2007; 8:302–30. [PubMed: 17468046]
67. Abou-Khalil, B.; Musilus, KE. Atlas of EEG & Seizure Semiology. Elsevier; 2006.
68. Schwilden H, Schuttler J, Stoeckel H. Closed-loop feedback control of methohexital anesthesia by quantitative EEG analysis in humans. Anesthesiology. 1987; 67:341–7. [PubMed: 3631609]
69. Drummond JC, Brann CA, Perkins DE, Wolfe DE. A comparison of median frequency, spectral edge frequency, a frequency band power ratio, total power, and dominance shift in the determination of depth of anesthesia. Acta Anaesthesiol Scand. 1991; 35:693–9. [PubMed: 1763588]
70. Hemmings HC Jr, Akabas MH, Goldstein PA, Trudell JR, Orser BA, Harrison NL. Emerging molecular mechanisms of general anesthetic action. Trends Pharmacol Sci. 2005; 26:503–10. [PubMed: 16126282]
71. Bai D, Pennefather PS, MacDonald JF, Orser BA. The general anesthetic propofol slows deactivation and desensitization of GABA(A) receptors. J Neurosci. 1999; 19:10635–46. [PubMed: 10594047]
72. Devor M, Zalkind V. Reversible analgesia, atonia, and loss of consciousness on bilateral intracerebral microinjection of pentobarbital. Pain. 2001; 94:101–12. [PubMed: 11576749]
73. Williams ST, Conte MM, Goldfine AM, Noirhomme Q, Gosseries O, Thonnard M, Beattie B, Hersh J, Katz DI, Victor JD, Laureys S, Schiff ND. Common resting brain dynamics indicate a possible mechanism underlying zolpidem response in severe brain injury. Elife. 2014; 2:e01157. [PubMed: 24252875]
74. McCarthy MM, Brown EN, Kopell N. Potential network mechanisms mediating electroencephalographic beta rhythm changes during propofol-induced paradoxical excitation. J Neurosci. 2008; 28:13488–504. [PubMed: 19074022]
75. Feldman JL, Del Negro CA. Looking for inspiration: new perspectives on respiratory rhythm. Nat Rev Neurosci. 2006; 7:232–42. [PubMed: 16495944]

76. Besch G, Liu N, Samain E, Pericard C, Boichut N, Mercier M, Chazot T, Pili-Floury S. Occurrence of and risk factors for electroencephalogram burst suppression during propofol-remifentanil anaesthesia. Br J Anaesth. 2011; 107:749–56. [PubMed: 21828343]
77. Redlich FC, Callahan A, Mendelson RH. Electroencephalographic changes after eye opening and visual stimulation. Yale J Biol Med. 1946; 18:367–76. [PubMed: 20982666]
78. Lee U, Ku S, Noh G, Baek S, Choi B, Mashour GA. Disruption of frontal-parietal communication by ketamine, propofol, and sevoflurane. Anesthesiology. 2013; 118:1264–75. [PubMed: 23695090]
79. Imas OA, Ropella KM, Ward BD, Wood JD, Hudetz AG. Volatile anesthetics disrupt frontal-posterior recurrent information transfer at gamma frequencies in rat. Neuroscience letters. 2005; 387:145–50. [PubMed: 16019145]
80. Jordan D, Ilg R, Riedl V, Schorer A, Grimberg S, Neufang S, Omerovic A, Berger S, Untergehrer G, Preibisch C, Schulz E, Schuster T, Schroter M, Spoormaker V, Zimmer C, Hemmer B, Wohlschlager A, Kochs EF, Schneider G. Simultaneous electroencephalographic and functional magnetic resonance imaging indicate impaired cortical top-down processing in association with anesthetic-induced unconsciousness. Anesthesiology. 2013; 119:1031–42. [PubMed: 23969561]
81. Rampil IJ, Lockhart SH, Eger EI 2nd, Yasuda N, Weiskopf RB, Cahalan MK. The electroencephalographic effects of desflurane in humans. Anesthesiology. 1991; 74:434–9. [PubMed: 2001021]
82. Amzica F. Basic physiology of burst-suppression. Epilepsia. 2009; 50(Suppl 12):38–9. [PubMed: 19941521]
83. Ching S, Purdon PL, Vijayan S, Kopell NJ, Brown EN. A neurophysiological-metabolic model for burst suppression. Proc Natl Acad Sci U S A. 2012; 109:3095–100. [PubMed: 22323592]
84. Mirsattari SM, Sharpe MD, Young GB. Treatment of refractory status epilepticus with inhalational anesthetic agents isoflurane and desflurane. Arch Neurol. 2004; 61:1254–9. [PubMed: 15313843]
85. Stecker MM, Cheung AT, Pochettino A, Kent GP, Patterson T, Weiss SJ, Bavaria JE. Deep hypothermic circulatory arrest: I. Effects of cooling on electroencephalogram and evoked potentials. Ann Thorac Surg. 2001; 71:14–21. [PubMed: 11216734]
86. Doyle PW, Matta BF. Burst suppression or isoelectric encephalogram for cerebral protection: evidence from metabolic suppression studies. Br J Anaesth. 1999; 83:580–4. [PubMed: 10673873]
87. Rossetti AO, Reichhart MD, Schaller MD, Despland PA, Bogousslavsky J. Propofol treatment of refractory status epilepticus: a study of 31 episodes. Epilepsia. 2004; 45:757–63. [PubMed: 15230698]
88. Hunter G, Young GB. Status epilepticus: a review, with emphasis on refractory cases. Can J Neurol Sci. 2012; 39:157–69. [PubMed: 22343147]
89. Lewis LD, Ching S, Weiner VS, Peterfreund RA, Eskandar EN, Cash SS, Brown EN, Purdon PL. Local cortical dynamics of burst suppression in the anaesthetized brain. Brain. 2013; 136:2727–37. [PubMed: 23887187]
90. Kroeger D, Amzica F. Hypersensitivity of the anesthesia-induced comatose brain. J Neurosci. 2007; 27:10597–607. [PubMed: 17898231]
91. Koenig MA, Kaplan PW, Thakor NV. Clinical neurophysiologic monitoring and brain injury from cardiac arrest. Neurol Clin. 2006; 24:89–106. [PubMed: 16443132]
92. Yamatogi Y, Ohtahara S. Early-infantile epileptic encephalopathy with suppression-bursts, Ohtahara syndrome; its overview referring to our 16 cases. Brain Dev. 2002; 24:13–23. [PubMed: 11751020]
93. Rampil I. Consciousness, awareness, and the clinician. Can J Anesth. 2003; 50:R1–R5.
94. Rampil IJ, Weiskopf RB, Brown JG, Eger EI 2nd, Johnson BH, Holmes MA, Donegan JH. I653 and isoflurane produce similar dose-related changes in the electroencephalogram of pigs. Anesthesiology. 1988; 69:298–302. [PubMed: 3415010]
95. Bruhn J, Bouillon TW, Shafer SL. Bispectral index (BIS) and burst suppression: revealing a part of the BIS algorithm. Journal of clinical monitoring and computing. 2000; 16:593–6. [PubMed: 12580235]
96. Voss L, Sleigh J. Monitoring consciousness: the current status of EEG-based depth of anaesthesia monitors. Best Pract Res Clin Anaesthesiol. 2007; 21:313–25. [PubMed: 17900011]

97. Shanechi MM, Chemali JJ, Liberman M, Solt K, Brown EN. A brain-machine interface for control of burst suppression in medical coma. Conf Proc IEEE Eng Med Biol Soc. 2013; 2013:1575–8. [PubMed: 24110002]

98. Chemali J, Ching S, Purdon PL, Solt K, Brown EN. Burst suppression probability algorithms: state-space methods for tracking EEG burst suppression. J Neural Eng. 2013; 10:056017. [PubMed: 24018288]

99. Sinner B, Graf BM. Ketamine. Handb Exp Pharmacol. 2008:313–33. [PubMed: 18175098]

100. Olney JW, Farber NB. Glutamate receptor dysfunction and schizophrenia. Arch Gen Psychiatry. 1995; 52:998–1007. [PubMed: 7492260]

101. Seamans J. Losing inhibition with ketamine. Nat Chem Biol. 2008; 4:91–3. [PubMed: 18202677]

102. Moghaddam B, Adams B, Verma A, Daly D. Activation of glutamatergic neurotransmission by ketamine: a novel step in the pathway from NMDA receptor blockade to dopaminergic and cognitive disruptions associated with the prefrontal cortex. J Neurosci. 1997; 17:2921–7. [PubMed: 9092613]

103. Cavazzuti M, Porro CA, Biral GP, Benassi C, Barbieri GC. Ketamine effects on local cerebral blood flow and metabolism in the rat. J Cereb Blood Flow Metab. 1987; 7:806–11. [PubMed: 3121648]

104. Strebel S, Kaufmann M, Maitre L, Schaefer HG. Effects of ketamine on cerebral blood flow velocity in humans. Influence of pretreatment with midazolam or esmolol. Anaesthesia. 1995; 50:223–8. [PubMed: 7717488]

105. Vollenweider FX, Leenders KL, Oye I, Hell D, Angst J. Differential psychopathology and patterns of cerebral glucose utilisation produced by (S)- and (R)-ketamine in healthy volunteers using positron emission tomography (PET). Eur Neuropsychopharmacol. 1997; 7:25–38. [PubMed: 9088882]

106. Jorm CM, Stamford JA. Actions of the hypnotic anaesthetic, dexmedetomidine, on noradrenaline release and cell firing in rat locus coeruleus slices. Br J Anaesth. 1993; 71:447–9. [PubMed: 8104450]

107. Nacif-Coelho C, Correa-Sales C, Chang LL, Maze M. Perturbation of ion channel conductance alters the hypnotic response to the alpha 2-adrenergic agonist dexmedetomidine in the locus coeruleus of the rat. Anesthesiology. 1994; 81:1527–34. [PubMed: 7992922]

108. Nelson LE, Lu J, Guo T, Saper CB, Franks NP, Maze M. The alpha2-adrenoceptor agonist dexmedetomidine converges on an endogenous sleep-promoting pathway to exert its sedative effects. Anesthesiology. 2003; 98:428–36. [PubMed: 12552203]

109. Nelson LE, Guo TZ, Lu J, Saper CB, Franks NP, Maze M. The sedative component of anesthesia is mediated by GABA(A) receptors in an endogenous sleep pathway. Nat Neurosci. 2002; 5:979–84. [PubMed: 12195434]

110. Saper CB, Scammell TE, Lu J. Hypothalamic regulation of sleep and circadian rhythms. Nature. 2005; 437:1257–63. [PubMed: 16251950]

111. Sherin JE, Elmquist JK, Torrealba F, Saper CB. Innervation of histaminergic tuberomammillary neurons by GABAergic and galaninergic neurons in the ventrolateral preoptic nucleus of the rat. J Neurosci. 1998; 18:4705–21. [PubMed: 9614245]

112. Morairty S, Rainnie D, McCarley R, Greene R. Disinhibition of ventrolateral preoptic area sleep-active neurons by adenosine: a new mechanism for sleep promotion. Neuroscience. 2004; 123:451–7. [PubMed: 14698752]

113. Espana RA, Berridge CW. Organization of noradrenergic efferents to arousal-related basal forebrain structures. J Comp Neurol. 2006; 496:668–83. [PubMed: 16615125]

114. Akeju O, Loggia ML, Catana C, Pavone KJ, Vazquez R, Rhee J, Contreras Ramirez V, Chonde DB, Izquierdo-Garcia D, Arabasz G, Hsu S, Habeeb K, Hooker JM, Napadow V, Brown EN, Purdon PL. Disruption of thalamic functional connectivity is a neural correlate of dexmedetomidine-induced unconsciousness. Elife. 2014; 4

115. Destexhe A, Contreras D, Steriade M. Mechanisms underlying the synchronizing action of corticothalamic feedback through inhibition of thalamic relay cells. J Neurophysiol. 1998; 79:999–1016. [PubMed: 9463458]

116. Nir Y, Staba RJ, Andrillon T, Vyazovskiy VV, Cirelli C, Fried I, Tononi G. Regional slow waves and spindles in human sleep. Neuron. 2011; 70:153–69. [PubMed: 21482364]

117. Antognini JF, Schwartz K. Exaggerated anesthetic requirements in the preferentially anesthetized brain. Anesthesiology. 1993; 79:1244–9. [PubMed: 8267200]

118. Lyon R, Feiner J, Lieberman JA. Progressive suppression of motor evoked potentials during general anesthesia: the phenomenon of "anesthetic fade". J Neurosurg Anesthesiol. 2005; 17:13–9. [PubMed: 15632537]

119. Andrews E. The oxygen mixture, a new anesthetic combination. Chicago Medical Examiner. 1868; 9:656–61.

120. Avramov MN, Shingu K, Mori K. Progressive changes in electroencephalographic responses to nitrous oxide in humans: a possible acute drug tolerance. Anesth Analg. 1990; 70:369–74. [PubMed: 2316879]

121. Hagihira S, Takashina M, Mori T, Mashimo T. The impact of nitrous oxide on electroencephalographic bicoherence during isoflurane anesthesia. Anesth Analg. 2012; 115:572–7. [PubMed: 22584553]

122. Jevtovic-Todorovic V, Todorovic SM, Mennerick S, Powell S, Dikranian K, Benshoff N, Zorumski CF, Olney JW. Nitrous oxide (laughing gas) is an NMDA antagonist, neuroprotectant and neurotoxin. Nat Med. 1998; 4:460–3. [PubMed: 9546794]

123. Niedermeyer, E.; da Silva, FL. EEG and Evoked Potentials in Neuroanesthesia, Intraoperative Neurological Monitoring, and Neurointensive Care, Electroencephalography: Basic Principles, Clinical Applications, and Related Fields. Lippincot, Williams & Wilkins; 2004. p. 1137-1164.

124. Moura LM, Shafi MM, Ng M, Pati S, Cash SS, Cole AJ, Hoch DB, Rosenthal ES, Westover MB. Spectrogram screening of adult EEGs is sensitive and efficient. Neurology. 2014; 83:56–64. [PubMed: 24857926]

125. Niedermeyer, E.; da Silva, FL. EEG Monitoring During Carotid Endarterectomy and Open Heart Surgery, Electroencephalography: Basic Principles, Clinical Applications, and Related Fields. Lippincot, Williams & Wilkins; 2004. p. 815-828.

126. Prerau MJ, Hartnack KE, Obregon-Henao G, Sampson A, Merlino M, Gannon K, Bianchi MT, Ellenbogen JM, Purdon PL. Tracking the sleep onset process: An empirical model of behavioral and physiological dynamics. PLoS Comput Biol. 2014; 10:e1003866. [PubMed: 25275376]

127. Sloan TB. Anesthetic effects on electrophysiologic recordings. J Clin Neurophysiol. 1998; 15:217–226. [PubMed: 9681559]

128. Franks NP, Lieb WR. Do general anaesthetics act by competitive binding to specific receptors? Nature. 1984; 310:599–601. [PubMed: 6462249]

129. Kelley, SD. Monitoring Consciousness: Using the Bispectral Index. Second. Boulder, CO: Covidien; 2010. p. 6

130. Bronez T. On the performance advantage of multitaper spectral analysis. IEEE Transactions on Signal Processing. 2002; 40:2941–2946.

131. Purdon PL, Brown EN. Clinical Electroencephalography for the Anesthesiologist, Partners Healthcare Office of Continuing Professional Development. A new approach to reading the EEG developed specifically for anesthesiology. 2014 3 CME credits, no cost to participants.

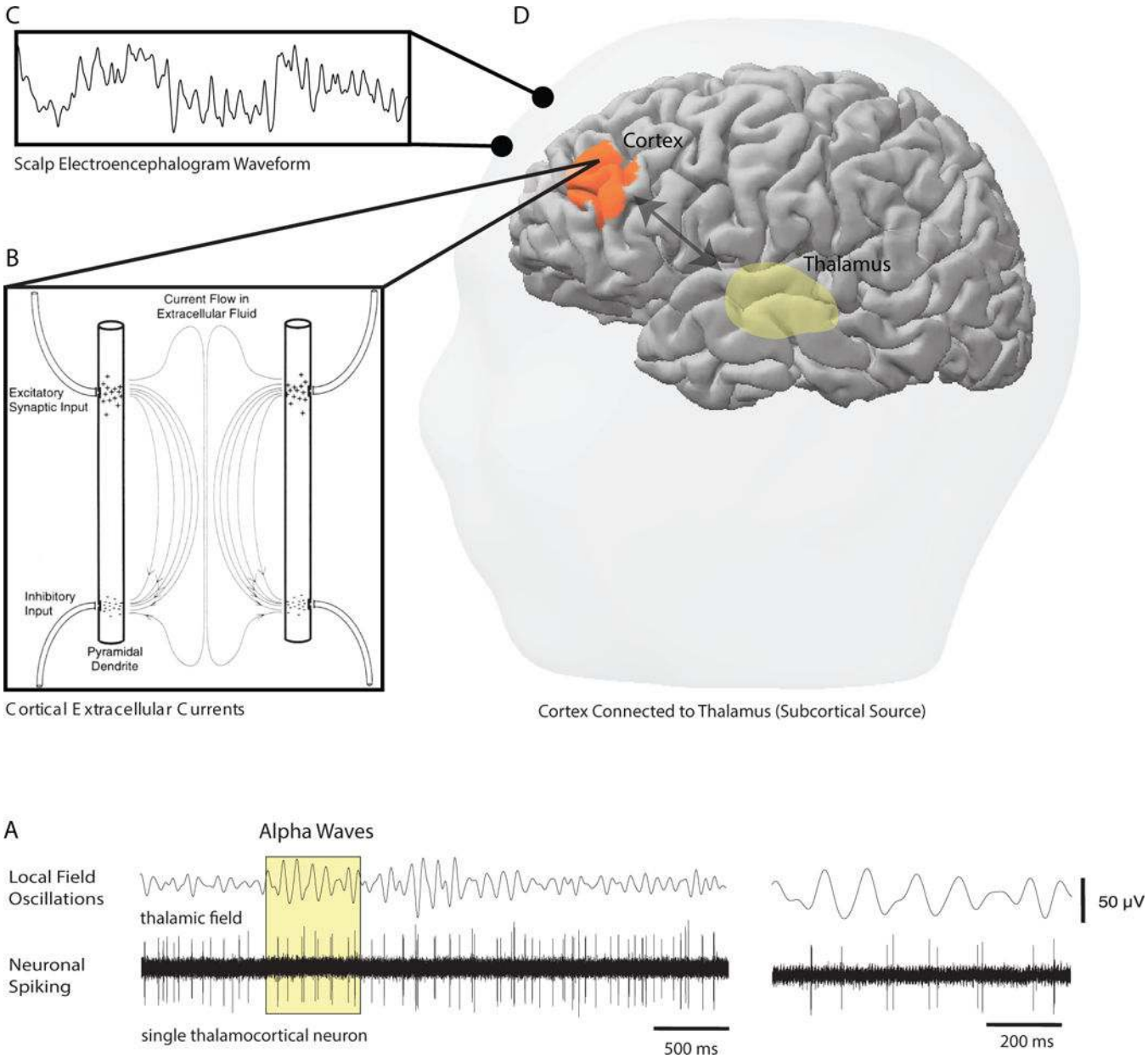

Fig. 1.

The neurophysiological origins of the electroencephalogram. A. Normal communication in the brain through neuronal spiking activity induces oscillatory extracellular electrical currents and potentials that are one of the ways information exchange is modulated and controlled in the central nervous system. B. The geometry of the neurons in the cortex favors the production of large extracellular currents and potentials. C. The electroencephalogram recorded on the scalp is a continuous measure of the electrical potentials produced in the cortex. D. Because the cortex (orange region) is highly interconnected with subcortical regions, such as the thalamus (yellow region), and the major arousal centers in the basal forebrain, hypothalamus, midbrain and pons, profound changes in neural activity in these areas can result in major changes in the scalp electroencephalogram. Panel A is reproduced

with permission from Hughes and Crunelli, *Neuroscientist*, 2005. Panel B is reproduced with permission from Rampil, *Anesthesiology*, 1998.

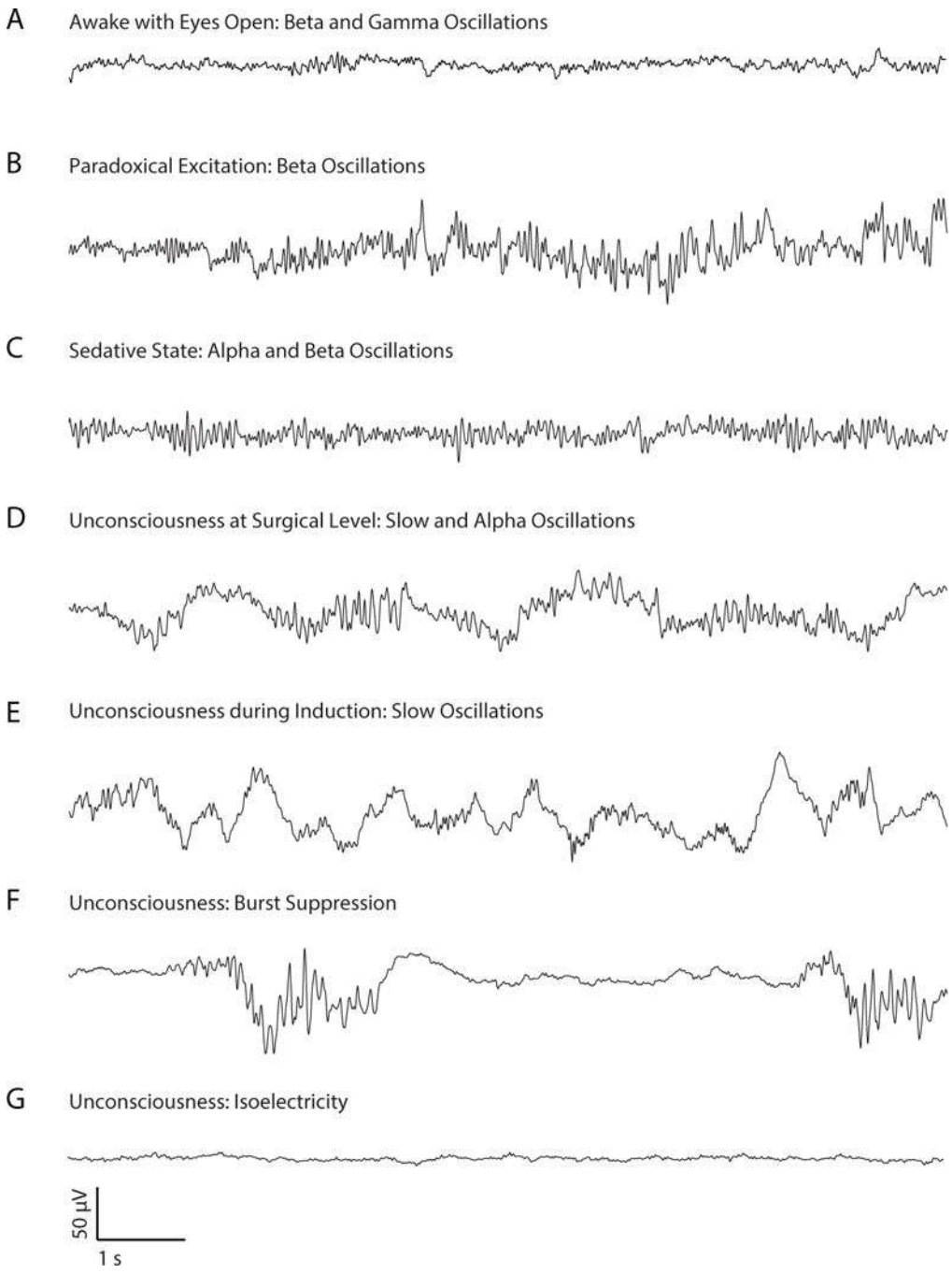

Fig. 2.

Unprocessed electroencephalogram signatures of propofol-induced sedation and unconsciousness. A. Awake eyes open electroencephalogram pattern. B. Paradoxical excitation. C. Alpha and beta oscillations commonly observed during propofol-induced sedation (Fig. 5). D. Slow-delta and alpha oscillations commonly seen during unconsciousness. E. Slow oscillations commonly observed during unconsciousness at induction with propofol (fig. 6) and sedation with dexmedetomidine (fig. 11) and with nitrous oxide (fig. 13). F. Burst suppression, a state of profound anesthetic-induced brain

inactivation commonly occurring in elderly patients,[76] anesthetic-induced coma and profound hypothermia (fig. 6B and 6D) G. Isoelectric electroencephalogram pattern commonly observed in anesthetic-induced coma and profound hypothermia. With the exception of the isoelectric state, the amplitudes of the electroencephalogram signatures of the anesthetized states are larger than the amplitudes of the electroencephalogram in the awake state by a factor of 5 to 20. All electroencephalogram recordings are from the same subject.

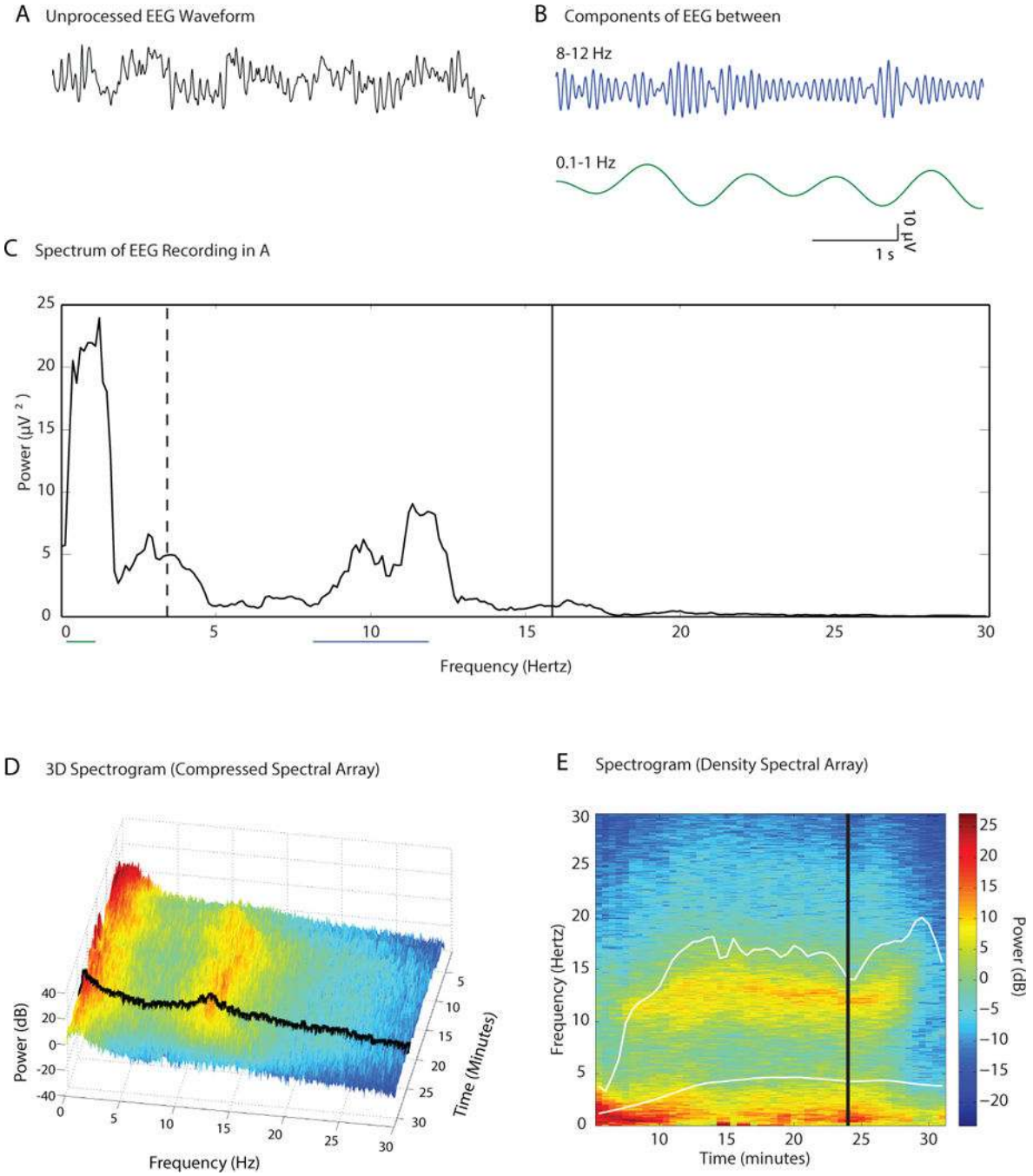

Fig. 3.

Construction of the spectrogram. A. A ten-second electroencephalogram trace recorded under propofol-induced unconsciousness. B. The electroencephalogram trace in A filtered into its two principal oscillations: the blue curve, an alpha (8 to 12 Hz) oscillation and the green curve, a slow-delta (0.1 to 4 Hz) oscillation. C. The spectrum provides a decomposition of the electroencephalogram in A in to power by frequency for all of the frequencies in a specified range. The range here is 0.1 to 30 Hz. Power at a given frequency is defined in decibels as the 10 times the log base 10 of the squared amplitude (10 $\log_{10}$

(amplitude)^2). The green horizontal line underscores the slow-delta frequency band and the blue horizontal line underscores the alpha frequency band used to compute the filtered signals in B. The median frequency, 3.4 Hz, (dashed vertical line) is the frequency that divides the power in the spectrum in half. The spectral edge frequency, 15.9 Hz (solid vertical line) is the frequency such that 95% of the power in the spectrum lies below this value. D. The three-dimensional spectrogram (compressed spectral array) displays the successive spectra computed on a 32-minute electroencephalogram recording from a patient anesthetized with propofol. Each spectrum is computed on a 3-second interval and adjacent spectra have 0.5 seconds of overlap. The black curve at minute 24 is the spectrum in C. D. The spectrogram in C plotted in two-dimensions (density spectral array). The black vertical curve is the spectrum in C. The lower white curve is the time course of the median frequency and the upper white curve is the time course of the spectral edge frequency. Panels A–E were adapted from Purdon and Brown, *Clinical Electroencephalography for the Anesthesiologist* (2014), with permission from the Partners Healthcare Office of Continuing Professional Development.[131]

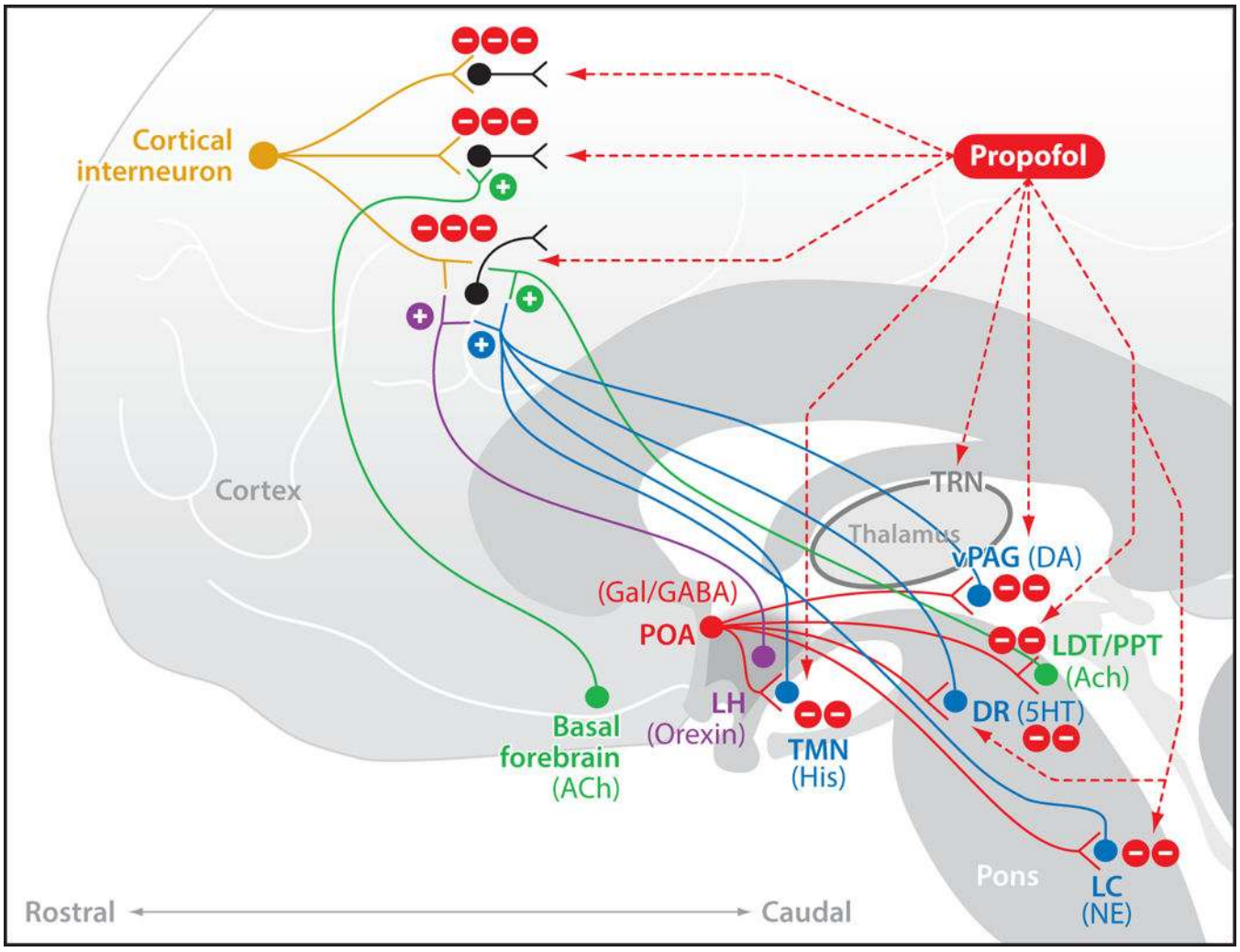

Fig. 4.

Neurophysiological mechanisms of propofol's actions in the brain. Propofol enhances $GABA_A$-mediated inhibition in the cortex, thalamus and brainstem. Shown are three major sites of action: post-synaptic connections between inhibitory interneurons and excitatory pyramidal neurons in the cortex; the GABAergic neurons in the thalamic reticular nucleus (TRN) of the thalamus; and post-synaptic connections between GABAergic projections from the pre-optic area (POA) of the hypothalamulus, and the monoaminergic nuclei which are the tuberomammillary nucleus (TMN) that releases histamine (His), the locus ceruleus (LC), that releases norepinephrine (NE), the dorsal raphé (DR) that releases serotonin (5HT); and the cholinergic nuclei which are the basal forebrain (BF), pedunculopontine tegmental (PPT) nucleus and the lateral dorsal tegmental (LDT) nucleus that release acetylcholine (Ach). This figure is reproduced with permission from Brown, Purdon and Van Dort, *Annual Review of Neuroscience*, 2011.

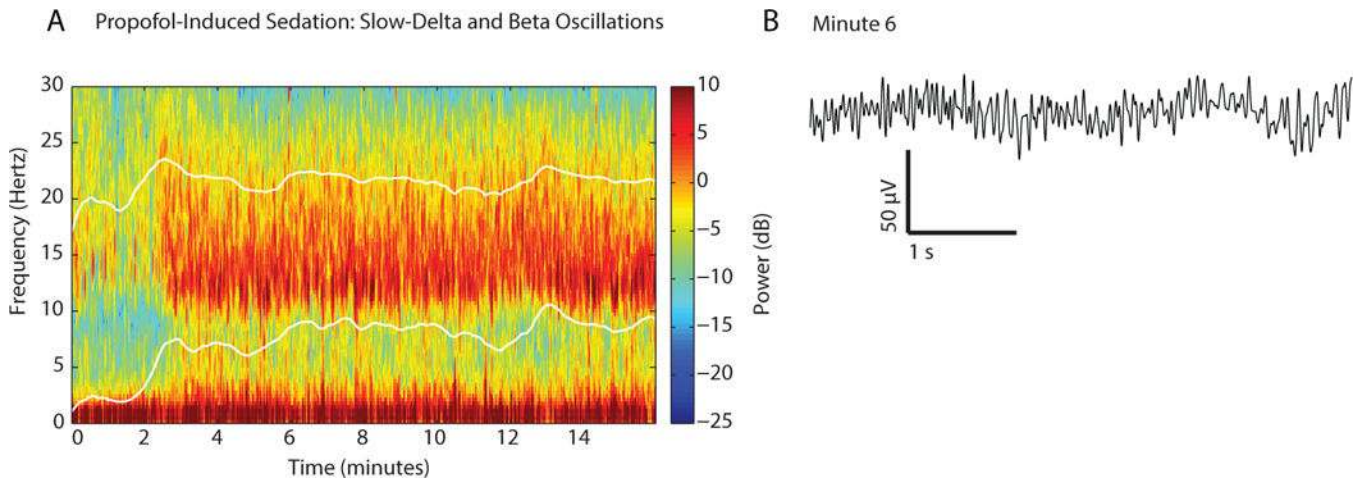

Fig. 5.

Spectrogram and the time-domain signature of propofol-induced sedation. A. Spectrogram shows slow-delta oscillations (0.1 to 4 Hz) and alpha-beta (8 to 22 Hz) oscillations in a volunteer subject receiving a propofol infusion to achieve and maintain a target effect-site concentration of 2 mcg/ml, starting at time zero.[20] The subject was responding correctly to the verbal, but not to click train auditory stimuli delivered every 4-seconds for the entire 16 minutes suggesting that she was becoming sedated.[20] The lower and upper white curves are the median and the spectral edge frequencies respectively. B. Ten-second electroencephalogram trace recorded at minute 6 of the spectrogram in A.

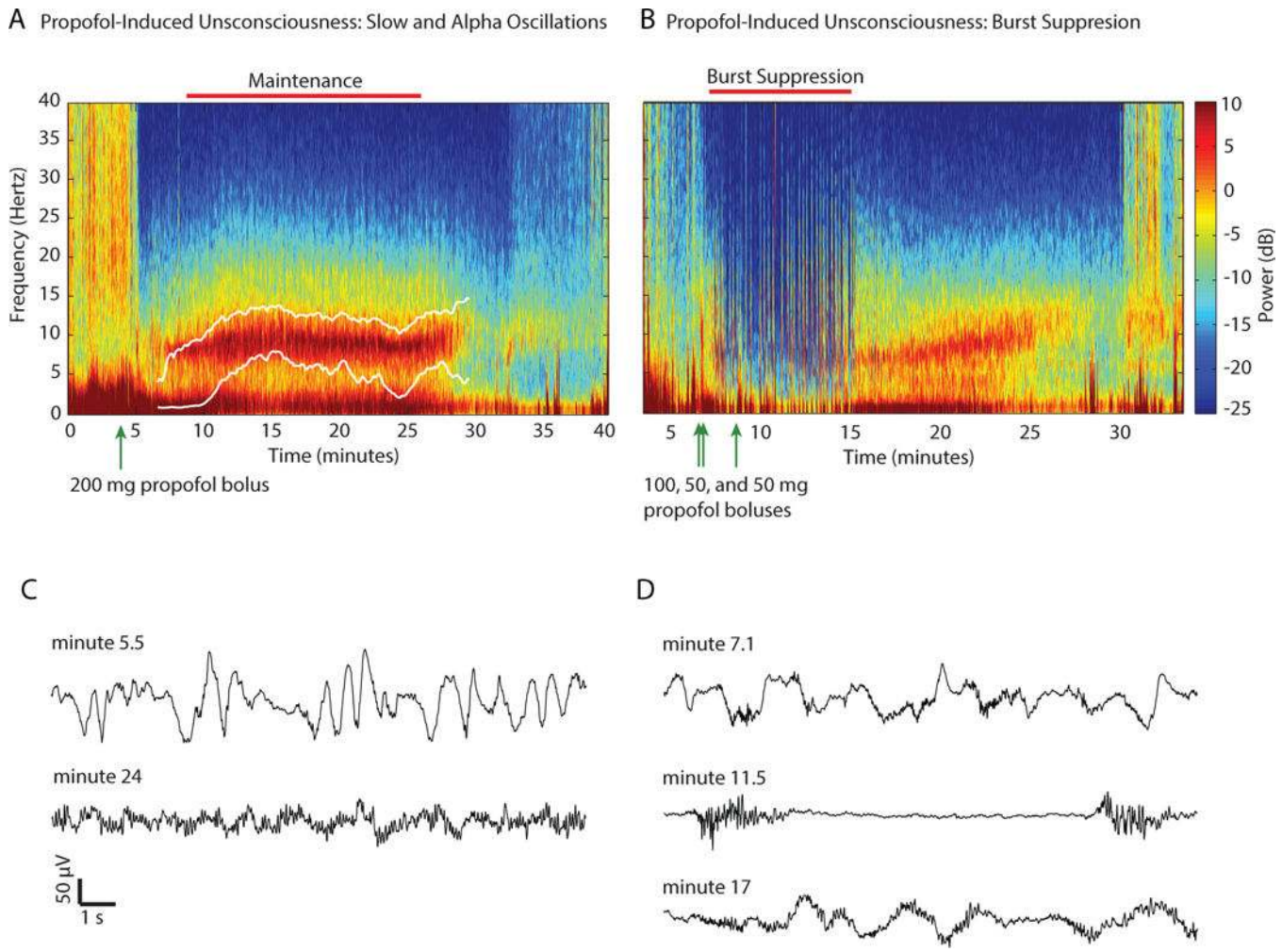

Fig. 6.

Spectrogram and time-domain electroencephalogram signatures of two patients receiving propofol for induction and maintenance of unconsciousness. A. High slow-delta power following the 200mg propofol bolus at minute 3 is evident between minutes 3 and 5. The electroencephalogram transitions to robust slow-delta and alpha oscillations maintained by a propofol infusion at 100mcg/kg/min. The lower and upper white curves are the median and the spectral edge frequencies respectively. B. Following bolus doses of propofol the patient's electroencephalogram transitions between 3 different states: slow oscillations (minutes 5 to 8) following the 100 mg propofol bolus at minute 3; burst suppression (minutes 8 to 15) following two additional 50 mg propofol boluses; and slow-delta and alpha oscillations from minutes 15 to 25. Beginning at minute 24 the alpha band power decreases and broadens to the beta band. The slow-delta oscillation power decreases after minute 24. The dissipation of the slow-delta and alpha oscillation power as the patient emerges gives the appearance of a zipper opening. C. Ten-second electroencephalogram traces recorded at minute 5.5 (slow-delta oscillations) and minute 24 (slow-delta and alpha oscillations) of the spectrogram in A. D. Ten-second electroencephalogram traces showing slow oscillations at minute 7.1, burst suppression at minute 11.5 and slow-delta and alpha oscillations at minute 17 for the spectrogram in B. Panels A–D were adapted from Purdon

and Brown, *Clinical Electroencephalography for the Anesthesiologist* (2014), with permission from the Partners Healthcare Office of Continuing Professional Development.[131]

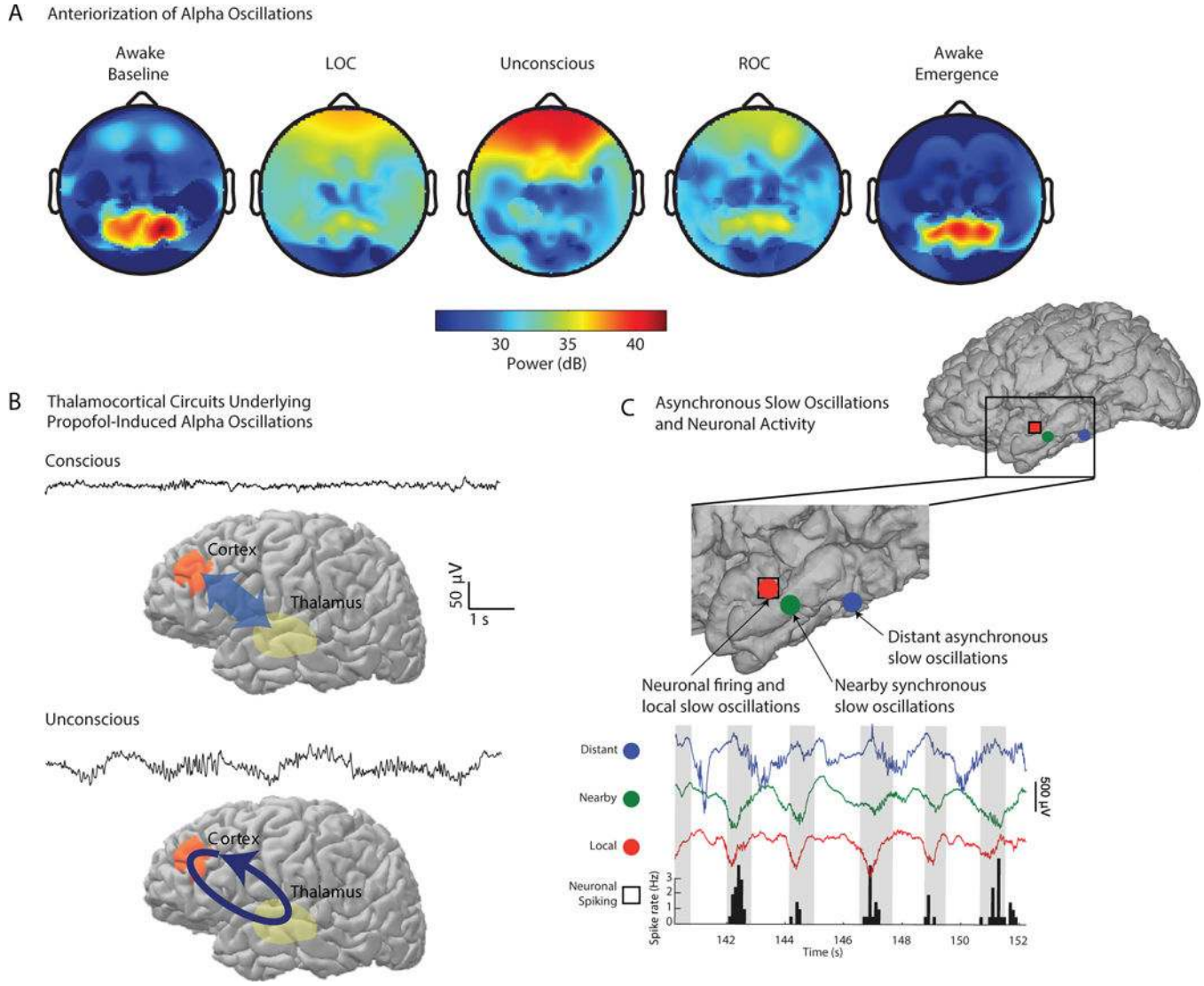

Fig. 7.

Spatio-temporal characterization of electroencephalogram alpha and slow oscillations observed during induction of and recovery from propofol-induced unconsciousness. A. In the volunteer subject lying awake with eyes closed, spatially coherent alpha oscillations are observed over the occipital area. The alpha oscillations shift to the front of the head with loss of consciousness (LOC) where they intensify and become spatially coherent during unconsciousness. The alpha oscillations dissipate anteriorly and return to the occipital area during return of consciousness (ROC) where they re-intensify and are spatially coherent in the eyes-closed awake state. B. During consciousness there is broadband communication between the thalamus and the frontal cortex with beta and gamma activity in the electroencephalogram. Modeling studies suggest during propofol-induced unconsciousness that the spatially coherent alpha oscillations are highly-structured rhythms in thalamocortical circuits.[57] C. Slow oscillations recorded from grid electrodes implanted in a patient with epilepsy, 30 seconds after bolus induction of general anesthesia with propofol. The slow oscillations at nearby electrodes (red and green dots) are in phase (red and green traces)

whereas the slow oscillation recorded at an electrode 2 centimeters away (blue dot) is out of phase (blue trace) with those at the other two locations. Neurons spike only (histograms) in a limited time window governed by the phase of the local slow oscillations. These slow oscillations are a marker of intracortical fragmentation with propofol as communication through spiking activity is restricted to local areas. The spatially coherent alpha oscillations and the disruption of neural spiking activity associated with the slow oscillations are likely to be two of the mechanisms through which propofol induces unconsciousness. Panel A is reproduced from Purdon et al. *PNAS*, 2013 and Panel B is adapted from Lewis et al. *PNAS*, 2012 with permission.

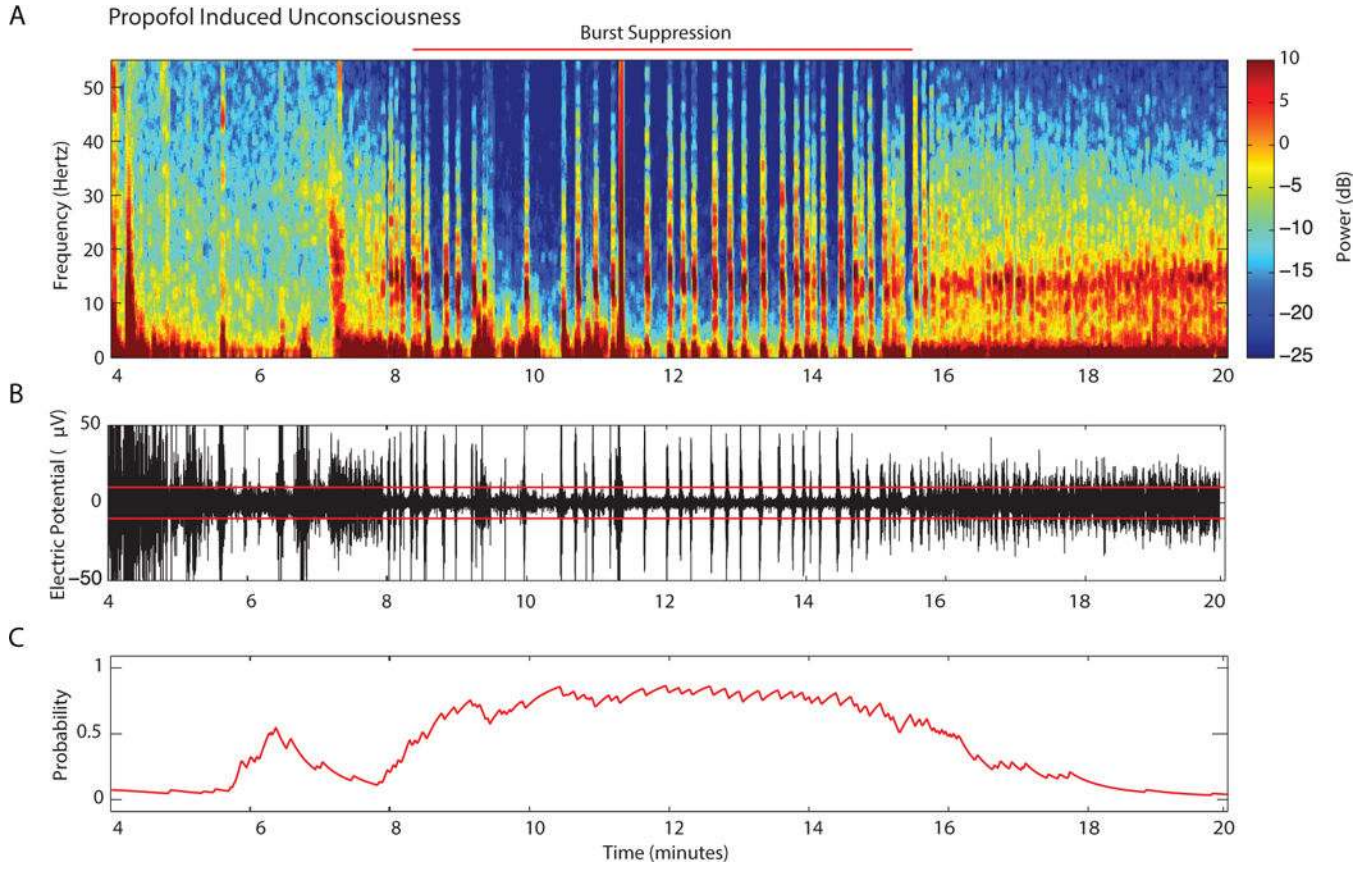

Fig. 8.

Characterization of burst suppression. A. The spectrogram in fig. 6B from minute 4 to minute 20. Burst suppression in the spectrogram shows as periods of blue (isoelectric activity) interspersed with periods of red-yellow (slow-delta and alpha oscillations). The horizontal red line shows the principal period of burst suppression. B. Unprocessed electroencephalogram recordings corresponding to the spectrogram in A. The horizontal red lines at ±5 microvolts are the thresholds which separate burst events (amplitude ≥5 microvolts) from suppression events (amplitude < 5 microvolts) C. The burst-suppression probability provides an estimate of the instantaneous probability of the electroencephalogram being suppressed.[97] Although it is apparent in the spectrogram and in the unprocessed electroencephalogram that the period of strong burst suppression extends from minute 8 to 16, the burst-suppression probability analysis shows that it does not completely subside until minute 17 as in Fig. 6B.

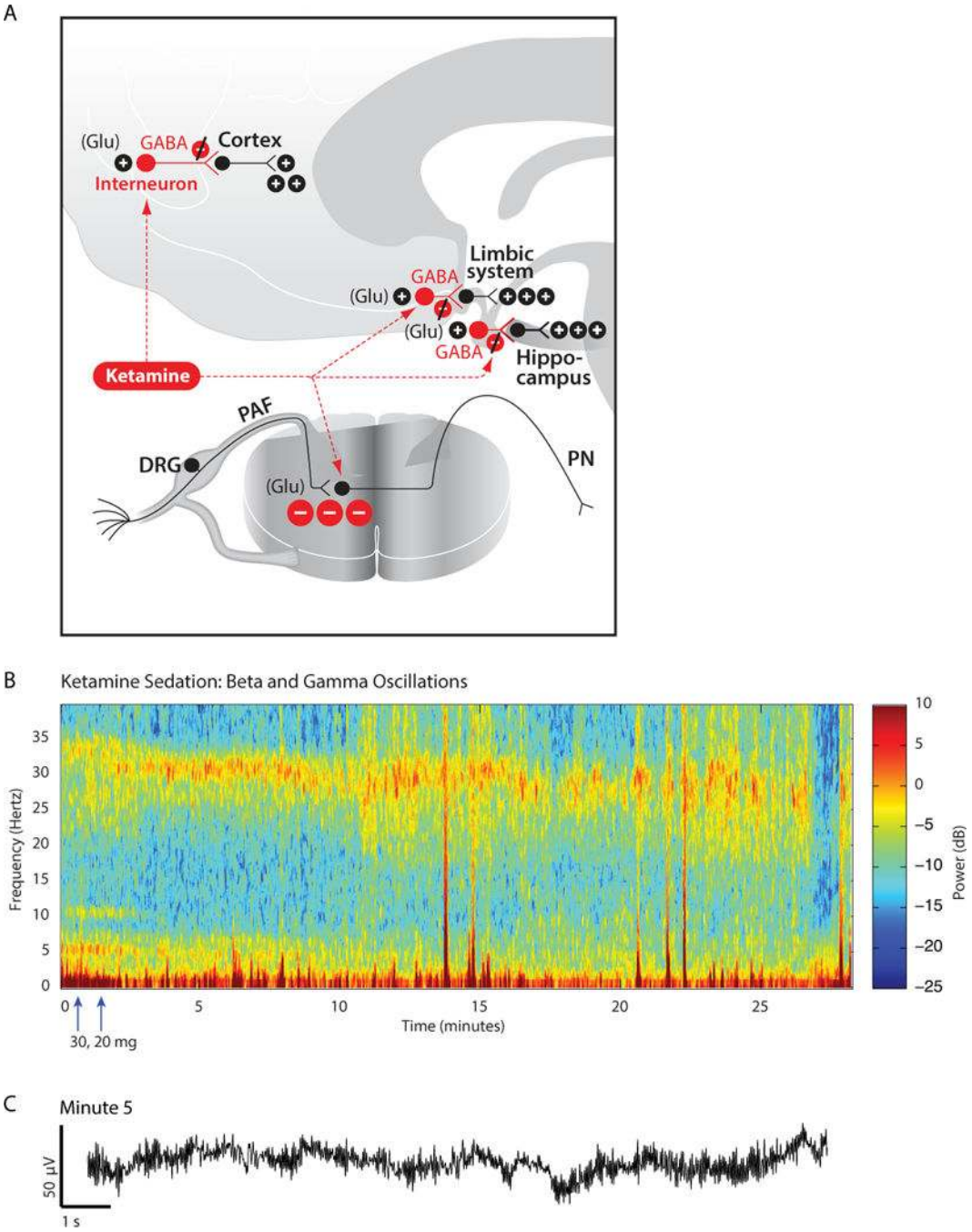

Fig. 9.

Neurophysiology and electroencephalogram signatures of ketamine. A. At low doses, ketamine blocks preferentially the actions of glutamate NMDA receptors on GABAergic inhibitory interneurons in the cortex and subcortical sites such as the hippocampus and the limbic system. The antinociceptive effect of ketamine is due in part to its blockade of glutamate release from peripheral afferent (PAF) neurons in the dorsal root ganglia (DRG) at their synapses on to projection neurons (PN) in the spinal cord. B. Spectrogram showing the beta-gamma oscillations in the electroencephalogram of a sixty-one year-old woman

who received ketamine sedation for a vacuum dressing change. Blocking the inhibitory action of the interneurons in cortical and subcortical circuits helps explain why ketamine produces a high-frequency beta oscillation as its electroencephalogram signature. C. Ten-second electroencephalogram trace recorded at minute 5 from the spectrogram in B. Arrows indicates times of ketamine doses. Panel A is reproduced with permission from Brown, Lydic and Schiff, *New England Journal of Medicine*, 2010. Panels B and C were adapted from Purdon and Brown, *Clinical Electroencephalography for the Anesthesiologist* (2014), with permission from the Partners Healthcare Office of Continuing Professional Development.[131]

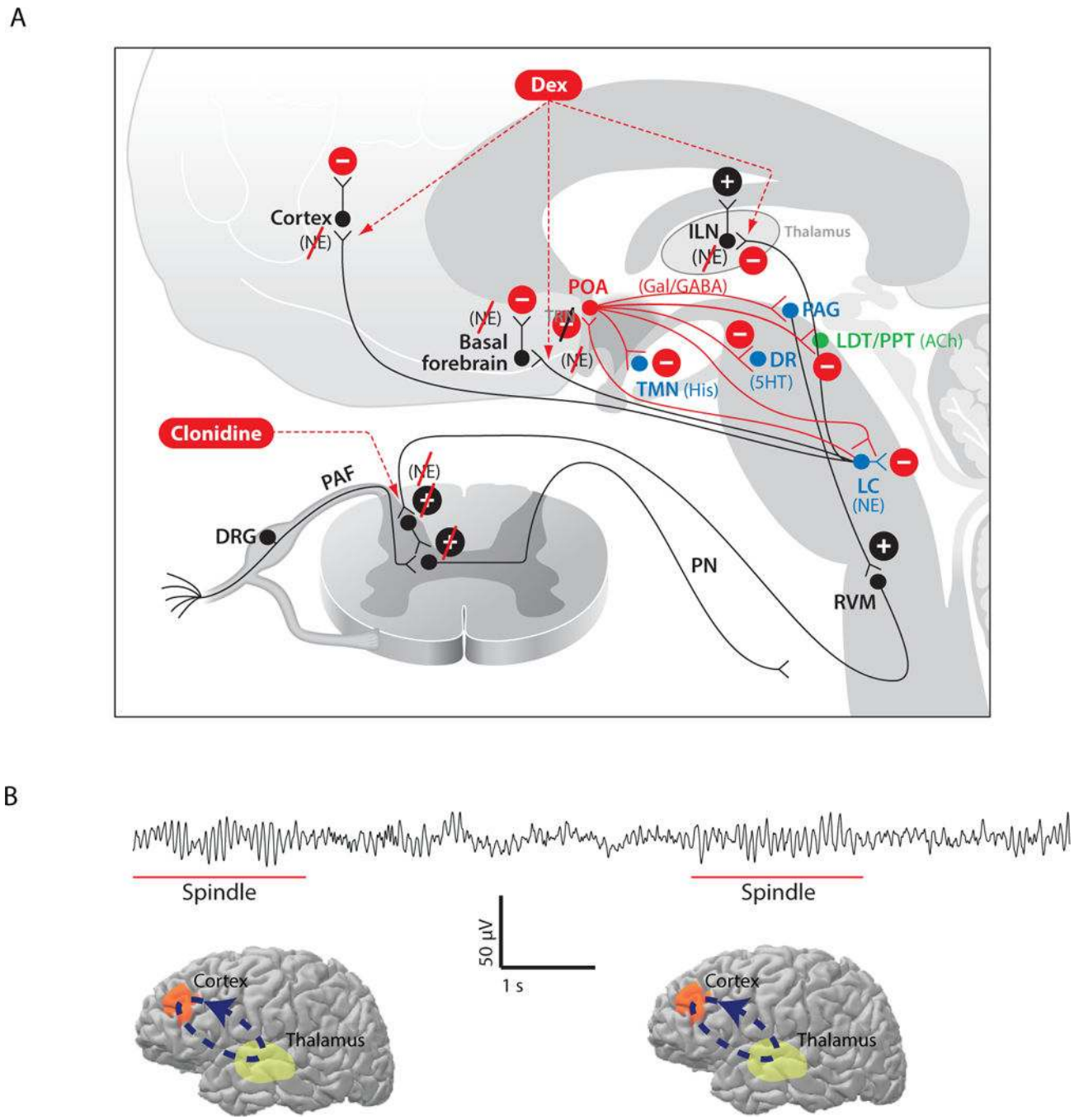

Fig. 10.

Neurophysiology of dexmedetomidine. A. Dexmedetomidine acts pre-synaptically to block the release of norepinephrine (NE) from neurons projecting from the locus coeruleus (LC) to the basal forebrain (BF), the pre-optic area (POA) of the hypothalamus, the intralaminar nucleus (ILN) of the thalamus and the cortex. Blocking the release of NE in the POA leads to activation of its inhibitory GABAergic (GABA) and galanergic (Gal) projections to dorsal raphé (DR) which releases serotonin (5HT), the tuberomamillary nucleus (TMN) which releases histamine (His), the LC, the ventral periacqueductal gray (PAG) which releases

dopamine, the lateral dorsal tegmental (LDT) nucleus and the pedunculopontine tegmental (PPT) nucleus which release acetylcholine (Ach). These actions lead to decreased arousal by inhibition of the arousal centers. B. Ten-second electroencephalogram segment showing spindles, intermittent 9 to 15 Hz oscillations (underlined in red), characteristic of dexmedetomidine sedation. C. The spindles are most likely produced by intermittent oscillations between the cortex and thalamus (light green region). Panel A is reproduced with permission from Brown, Purdon and Van Dort, *Annual Review of Neuroscience*, 2011.

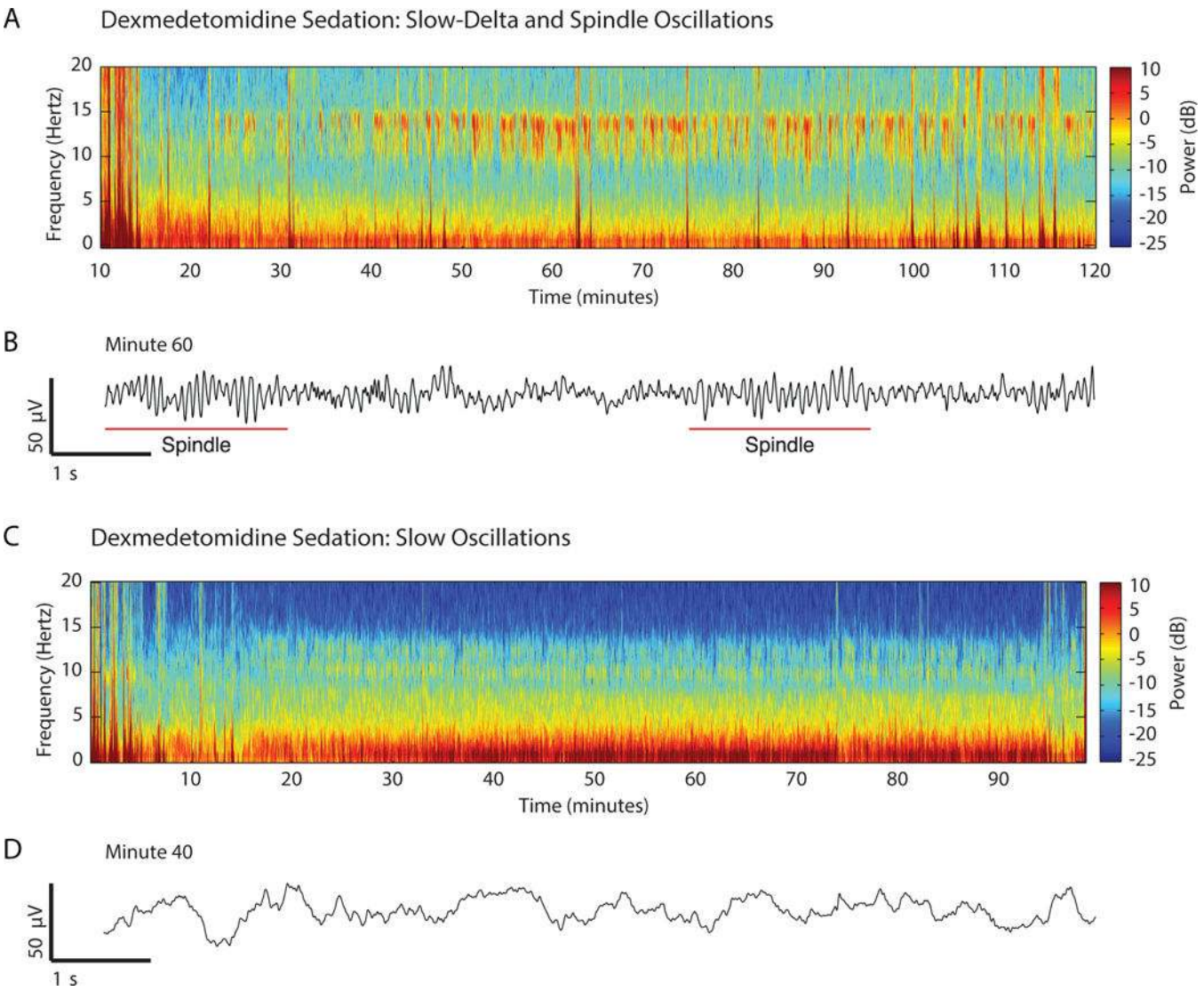

Fig. 11.

Spectrograms and time-domain electroencephalogram signatures of dexmedetomidine-induced sedation. A. Spectrogram of a 59 kg patient receiving a 0.65 mcg/kg/hour dexmedetomidine infusion to maintain sedation. The spectrogram shows spindles (9 to 15 Hz oscillations) and slow-delta oscillations. B. Ten-second electroencephalogram trace recorded at minute 60 from the spectrogram in A emphasizing spindles (red underlines). C. Spectrogram of a 65 kg patient receiving a 0.85 mcg/kg/hour dexmedetomidine infusion to maintain sedation. D. Ten-second electroencephalogram trace recorded at minute 40 from the spectrogram in C showing the slow-delta oscillations. Panels A–D were adapted from Purdon and Brown, *Clinical Electroencephalography for the Anesthesiologist* (2014), with permission from the Partners Healthcare Office of Continuing Professional Development.[131]

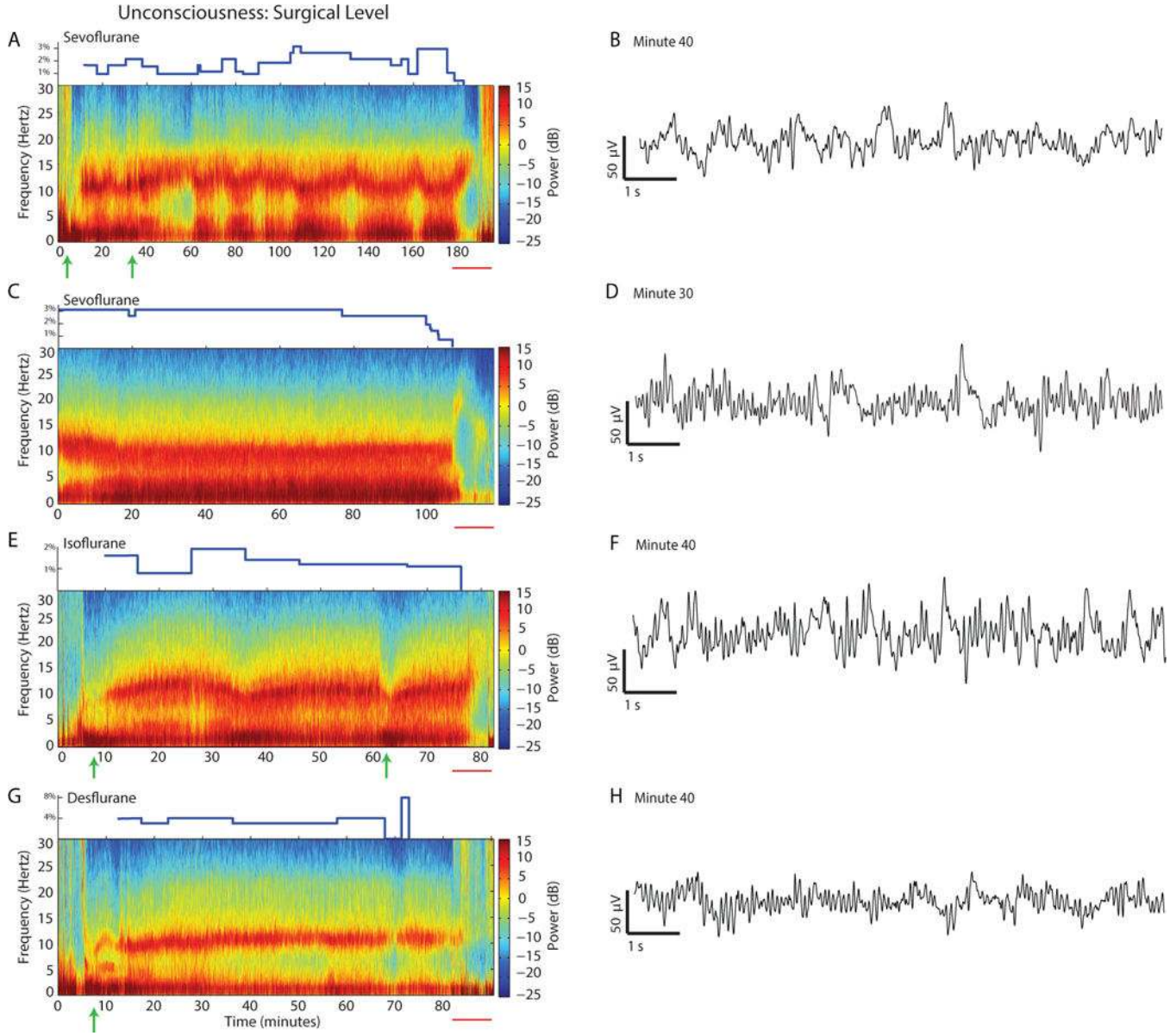

Fig. 12.

Spectrograms and time-domain electroencephalogram signatures of sevoflurane, isoflurane and desflurane at surgical levels of unconsciousness. The inspired concentration of the anesthetics is the blue trace in the upper part of each panel. Green arrows below each panel are propofol bolus doses. A. At sub-MAC concentrations (minute 40 to minute 60) the spectrogram of sevoflurane resembles that of propofol (fig. 6, A and B). As the concentration of sevoflurane is increased (minute 100 to minute 120), theta (5 to 7Hz) oscillations appear. The theta oscillations dissipate when the sevoflurane concentration (blue curve) is decreased. B. Ten-second electroencephalogram trace of sevoflurane recorded at minute 39.8 of the spectrogram in A. C. The spectrogram of sevoflurane shows constant the alpha, slow, delta and theta oscillations at a constant concentration of 3%. D. Ten-second electroencephalogram trace of sevoflurane recorded at minute 30 of the spectrogram in C. E.

At sub-MAC concentrations (minute 16 to minute 26) the spectrogram of isoflurane resembles that of propofol (fig. 6A, B) and sub-MAC sevoflurane (panel A). Theta oscillations strengthen as the isoflurane concentration increases towards MAC. F. Ten-second electroencephalogram trace of desflurane recorded at minute 40 of the spectrogram in E. G. At the sub-MAC concentrations shown here the spectrogram of desflurane resembles propofol with very low theta oscillation power. H. Ten-second electroencephalogram trace of desflurane recorded at minute 40 of the spectrogram in G. Panels A, C, E, and G were adapted from Purdon and Brown, *Clinical Electroencephalography for the Anesthesiologist* (2014), with permission from the Partners Healthcare Office of Continuing Professional Development.[131]

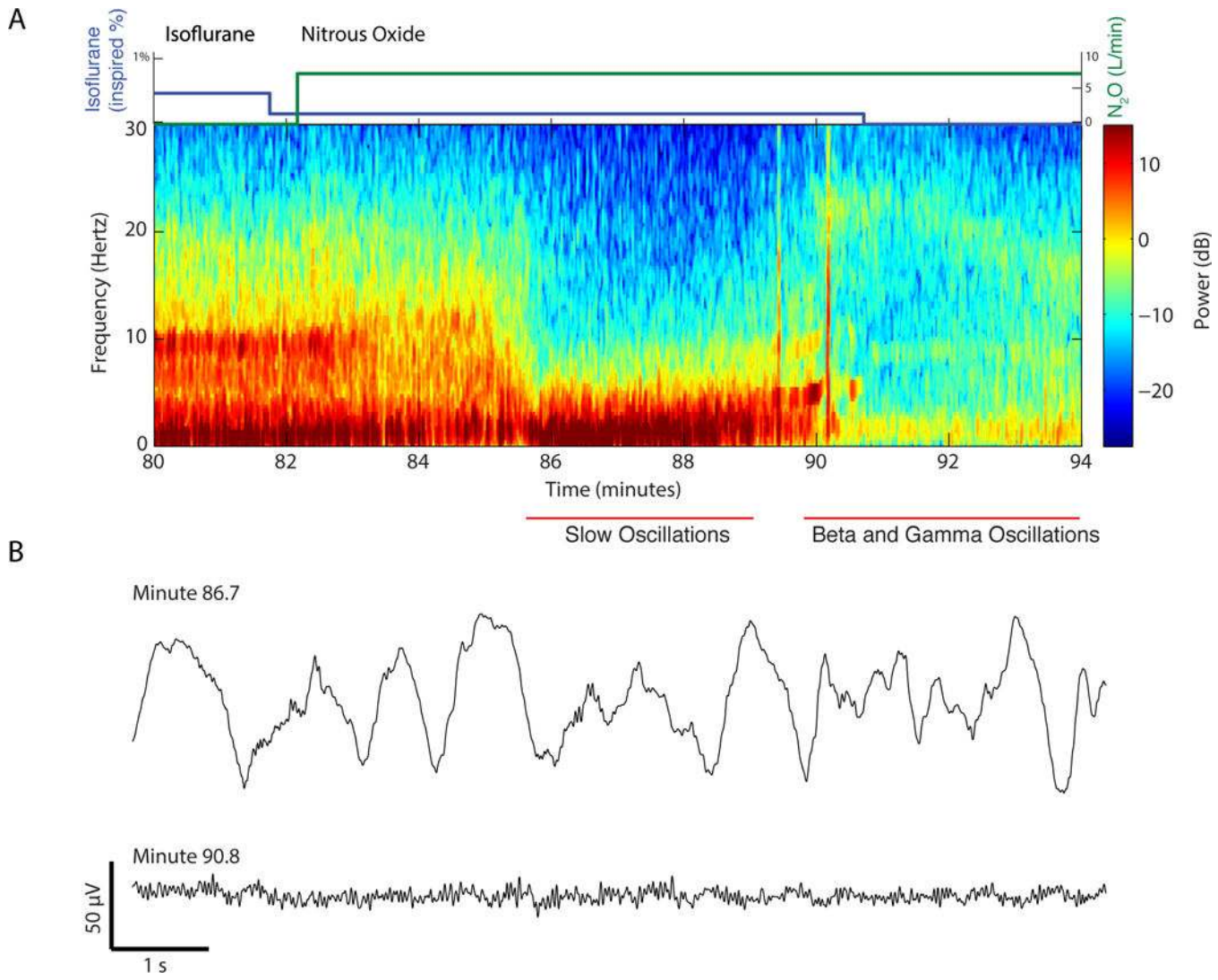

Fig. 13.

Slow-delta and beta-gamma oscillations associated with nitrous oxide. A. In anticipation of emergence, a patient was maintained on 0.5% isoflurane and 58% oxygen. At minute 82, the composition of the anesthetic gases was changed to 0.2% isoflurane (blue curve) in 75% nitrous oxide (green curve) and 24% oxygen. The total gas flow was increased from 3 to 7 liters per minute. The alpha, theta and slow oscillation power decreased between minutes 83 to 85. At minute 86 the power in the theta to beta bands decreased considerably (blue area) as the slow-delta oscillation power increased. At minute 88 the slow-delta oscillation power decreased and the beta-gamma oscillations appeared at minute 90. The flow rates and anesthetic concentrations were maintained constant between minutes 82 and 91. Isoflurane was turned off at minute 91. B. Ten-second electroencephalogram traces of the slow-delta oscillation at minute 86.7 and the beta-gamma oscillations at minute 90.8. Panels A and B were adapted from Purdon and Brown, *Clinical Electroencephalography for the Anesthesiologist* (2014), with permission from the Partners Healthcare Office of Continuing Professional Development.[131]

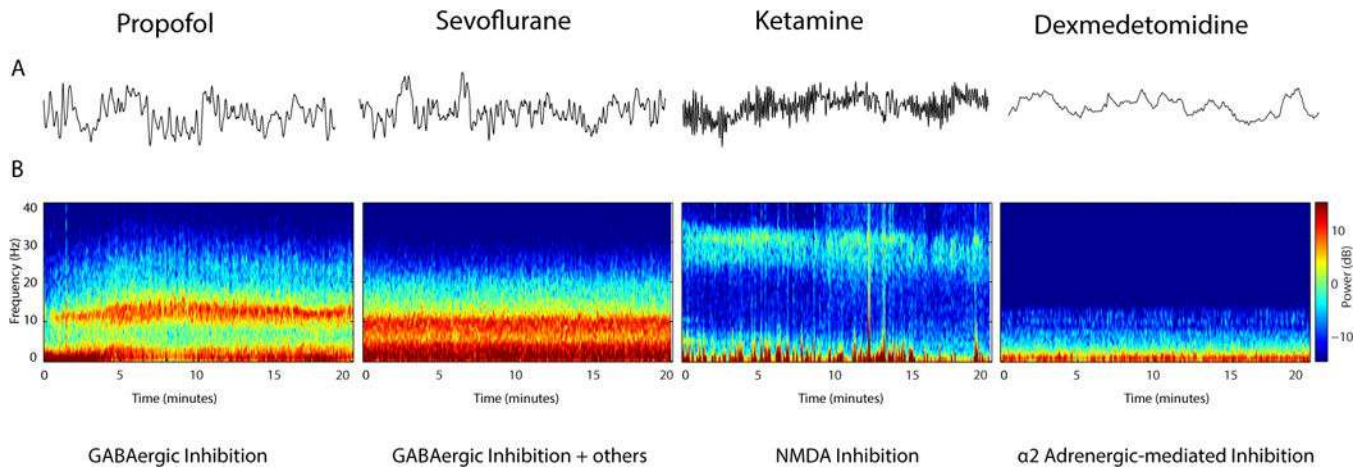

Fig. 14.

Different anesthetics (propofol, sevoflurane, ketamine and dexmedetomidine), different electroencephalogram signatures and different molecular and neural circuit mechanisms. A. Anesthetic-specific differences in the electroencephalogram are difficult to discern in unprocessed electroencephalogram waveforms. B. In the spectrogram, it is clear that different anesthetics produce different electroencephalogram signatures. The dynamics the electroencephalogram signatures can be related to the molecular targets and the neural circuits at which the anesthetics act to create altered states of arousal. Panels A and B were adapted from Purdon and Brown, *Clinical Electroencephalography for the Anesthesiologist* (2014), with permission from the Partners Healthcare Office of Continuing Professional Development.[131]

Table 1

Spectral Frequency Bands

Name	Frequency Range (Herz, cycles per seconds)
Slow	< 1
Delta	1–4
Theta	5–8
Alpha	9–12
Beta	13–25
Gamma	26–80